Accepted Manuscript

Geological Society, London, Memoirs

A review of mantle xenoliths in volcanic rocks from southern Victoria Land, Antarctica

A. P. Martin, A. F. Cooper, R. C. Price, C. L. Doherty & J. A. Gamble

DOI: https://doi.org/10.1144/M56-2019-42

To access the most recent version of this article, please click the DOI URL in the line above. When citing this article please include the above DOI.

Received 28 November 2019
Revised 3 April 2021
Accepted 5 April 2021

Supplementary material at https://doi.org/10.6084/m9.figshare.c.5407260

A review of mantle xenoliths in volcanic rocks from southern Victoria Land, Antarctica

A. P. Martin[1], A. F. Cooper[2], R. C. Price[3], C. L. Doherty[4], Gamble, J. A.[5,6]

[1] GNS Science, Private Bag 1930, Dunedin, New Zealand

[2] Department of Geology, University of Otago, P.O. Box 56, Dunedin, New Zealand

[3] Science and Engineering, University of Waikato, Hamilton, New Zealand

[4] Environmental and Occupation Health Sciences Institute, Rutgers University, Piscataway, NJ 08854, USA

[5] School of Geography, Environment and Earth Sciences, Victoria University of Wellington, Wellington, New Zealand;

[6] School of Biological, Earth and Environmental Science, University College Cork, Cork, Ireland

Abstract

Mantle xenoliths from southern Victoria Land have been collected and extensively studied for over a century. In this chapter, chemical and petrological data are, for the first time, comprehensively collated and petrogenetic models for the regional mantle are reviewed and assessed. The most common lithologies are spinel lherzolite and harzburgite; plagioclase lherzolite also occurs, and pyroxenite xenoliths found across the province comprise < 20 % of all mantle xenoliths. The lithospheric mantle in the region has Palaeoproterozoic stabilization ages, though pockets of younger mantle may exist. This peridotite mantle comprises a HIMU-component *sensu stricto*, has been variably carbonated and has undergone multiple melt-depletion events. Regional variations in a sedimentary (EMI) component to the west, and iron-rich components to the east, reflect a complex history of refertilisation and metasomatism. The sources of these fluids are likely to have been oceanic crust subducted during c. 0.5 Ga and older events. Peridotites have been cross-cut by pyroxenite veins, probably in multiple episodes, with the geochemistry of some samples reflecting the involvement of an upper continental crust (EMII) component. Future research directions should

apply advanced isotopic, noble gas and volatile techniques to better understand the upper mantle below this dynamic rifting environment.

Introduction

In many alkalic volcanic provinces fragments of the mantle are entrained as xenoliths in the ascending melts. Such xenoliths record conditions in the upper mantle relevant to understanding igneous petrogenesis, glacial isostatic adjustment and regional tectonics; they also place boundary conditions on remotely and geophysically sensed data. At many locations across a continental rift shoulder in southern Victoria Land, Antarctica, Cenozoic alkalic volcanic rocks are hosts to mantle xenoliths (Fig. 1). This region is of significant geological and petrological interest because: (a) mantle xenoliths and their host volcanic rocks have been intensively studied here for more than a century and, consequently, an extensive petrological and geochemical database can be compiled; (b) the region is the locus of active volcanism; (c) it is the site of continental rifting; (d) it is at the tectonic boundary between the West Antarctic Rift System and the Transantarctic Mountains and; (e) it is accessible from historic and modern Antarctic bases, which means it is an area where many petrological, geophysical and remotely sensed studies have been, and continue to be, focussed.

Mantle xenoliths were among some of the earliest geological specimens collected from Antarctica. Prior (1902, p.328) described

> *A large mass of basalt from Franklin Island is remarkable for the number and large size of the olivine-enstatite nodules…the olivine-nodules are as large as a fist…and consist of a fairly coarse-grained aggregate of pale greenish olivine, yellow enstatite showing polysynthetic twinning, brilliant green chrome-diopside, and pisolite.*

The first sketches of microscopic textures of mantle xenoliths from the region were published by Prior (1907), and the first chapter on mantle xenoliths by Thomson (1916) also contained the first published thin section photomicrographs. Many early works on mantle xenoliths were descriptive

(e.g. Smith 1954; Cole & Ewart 1968; McIver & Gevers 1970; Skinner et al. 1976). Forbes (1963) used mineral strain fabrics in mantle xenoliths to argue for a non-cognate origin (i.e. not genetically related to the host magma), but the first extensive overview of mantle xenoliths in the region was provided by Kyle et al. (1987). This Chapter builds on that seminal work. Since that time, reviews of specific mantle xenolith occurrences have been published for Foster Crater (Gamble & Kyle 1987; Gamble et al. 1988), White Island (Cooper et al. 2007; Martin et al. 2014a), Mount Morning (Martin et al. 2015a), Pipecleaner Glacier (Martin et al. 2014a) and Turtle Rock and Hut Point Peninsula (Niida 1988, 1990; Warner & Wasilewski 1995; Day et al. 2019).

In this Chapter, data for mantle xenoliths from this region, collected over more than a century, are collated and interpreted. This mantle setting is discussed and the implications for mantle petrogenesis are reviewed. The Chapter will not directly consider mantle conditions inferred from volcanic rocks as this has been the subject of recent reviews (Panter and Martin, this volume; Martin et al. 2021; Smellie & Martin 2021).

Geological Setting

The West Antarctic Rift System splits Antarctica, with the Transantarctic Mountains marking the rift's western shoulder (Fig. 1a; Tessensohn & Wörner 1991; Martin et al. 2015b; Tinto 2019). The Transantarctic Mountains comprise Precambrian to Cambrian metasedimentary (sedimentary rock that has been metamorphosed) lithologies cross-cut by mainly Cambrian to Ordovician granitic rocks of the Granite Harbour Intrusive Complex, which also includes the ultramafic lamprophyres of the Vanda Dykes (Gunn & Warren 1962; Wu & Berg 1992; Stump 1995; Cox et al. 2012). These older rocks are overlain by Devonian to Triassic Beacon Supergroup sedimentary-rocks (Barrett 1981) that are in turn intruded by the Jurassic Ferrar Dolerite (Burgess et al. 2015). Extension in the West Antarctic Rift System commenced in the Jurassic, with the major crustal-rifting phase occurring with Late Cretaceous Gondwana breakup (Siddoway 2008). A further extensional phase occurred in the Cenozoic along the western rift shoulder associated with significant crustal heating events until c.

100 Ma (Molzahn et al., 1999), coeval with Transantarctic Mountain uplift (Fitzgerald 2002). A third pulse of Paleogene extension was focussed in the Victoria Land Basin (Fig. 1b), an asymmetric graben along the western edge of the rift (Fitzgerald 2002; Fielding et al. 2006). Within the Victoria Land Basin, Neogene rifting has occurred primarily within the Terror Rift (Fig. 1b; Fielding et al. 2006; Martin & Cooper 2010), with some evidence for Quaternary activity (Hall et al. 2007). The Moho depth varies across the region from 40 km beneath the Transantarctic Mountains, shallowing eastwards to 18 km across the rift shoulder under the Ross Embayment (e.g. Wiens et al, this volume; McGinnis et al. 1985).

Cenozoic, alkalic volcanic rocks and hypabyssal intrusions, known collectively as the McMurdo Volcanic Group, have been emplaced along the western shoulder of the rift and in the foothills of the Transantarctic Mountains (Harrington 1958). The McMurdo Volcanic Group extends c. 2000 km between offshore Cape Adare in the north to Sheridan Bluff and Mount Early in the south (Fig. 1a; Kyle 1990). It has been sub-divided into three provinces, with the southernmost and the focus of this work, being the Erebus Volcanic Province in southern Victoria Land (Martin et al., 2021). This province is further divided into five volcanic fields, which are from north to south, Terror Rift, Ross Island, Mount Discovery, Mount Morning and Southern Local Suite (Fig. 2; Smellie and Martin, 2021). The discussion of data in this chapter are subdivided based on in which of the five volcanic fields the mantle xenoliths were brought to the surface. The volcanic rocks in the Erebus Volcanic Province were the earliest to be recognised as hosting mantle xenoliths (Prior 1902).

Methods

A compilation of published mineral and whole rock chemistry of mantle xenoliths of southern Victoria Land is provided in the extra supplementary material (ESM1). The method of analysis and the original reference is given for every single analysis (ESM1) to which the reader is referred for specific analysis parameters. For plotting, only data with appropriate totals, i.e. 100 ± 1 wt. % were used. Data with totals < 99 or > 101 wt.% are still included in ESM1 for completeness. The details of

the standard melting models used on figures in this Chapter and discussed in the text are also included in the ESM1.

For new analyses in this study, the following methods apply. Whole rock and electron microprobe analyses were undertaken in the Analytical Facility of Victoria University of Wellington (VUW), New Zealand. Major oxides and selected trace elements were determined using an Automated Philips PW-2002 X-ray fluorescence spectrometer with a Rhodium end-window tube. USGS and Japan samples were used as monitoring standards. Full details of the analytical methods are in Palmer (1990).

Electron microprobe analyses were undertaken on epoxy mounted, hand-picked mineral grains, polished and carbon coated and using the VUW Analytical Facility JEOL JXA-733 Superprobe electron microprobe microanalyser. Mineral analyses were made at 15kv accelerating voltage and a beam current of 1.2 x 10^{-8} A using synthetic oxides and natural minerals as standards. Analytical precision is approximately $\pm$ 1% for elements with an abundance of >10% and $\pm$ 5-10% for elements present in lower abundance.

Using the same epoxy mineral mounts, trace elements were determined by ArF Excimer Laser Ablation (Lambda Physik LPX 120i) coupled to a Fisons PlasmaQuad inductively coupled plasma – mass spectrometer in the Research School of Earth Sciences, Australian National University. Analytical procedures followed methods outlined in Eggins et al. (1997) NIST-610 glass and BHVO-1 were used as monitoring standards.

Results

Location of mantle xenoliths and other mantle rocks

The locations of all reported occurrences of mantle xenoliths in southern Victoria Land are shown on Figure 1, with the major references provided and prominent rock types summarised in Table 1. The locations where only crustal xenoliths have been found are reported in Kyle et al. (1987) and this

information is not replicated here. Additional information about localities where xenoliths have been searched for, and not found, is also included in Table 1. For example, no mantle xenoliths have been observed on Beaufort Island based on field exploration of the southern portion of the island (R. J. Moscati, *pers. comm.*), and no mantle-derived xenoliths have been reported in the Taylor Valley (Allibone et al. 1991). Other areas, such as the Dailey Islands or northern Beaufort Island have only been explored at a reconnaissance level and further study may reveal new mantle xenolith occurrences.

Sheridan Bluff and Mount Early (Fig. 1a), to the south of Erebus Volcanic Province, comprise McMurdo Volcanic Group rocks that have recently been mapped in detail and found not to contain mantle xenoliths or mantle-derived megacrysts (Panter 2021). The most primitive portions of the Ferrar Dolerite (e.g. Bédard et al. 2007) and the lamprophyric Vanda Dykes (Wu & Berg 1992) are beyond the scope of this chapter.

Petrography

Mantle xenoliths in the region are typically less than 10 cm in maximum dimension; however, much larger specimens (up to 1 m) have been documented (Fig. 3a). Peridotite and pyroxenite type xenoliths are commonly found together (Fig. 3b). The petrography of several mantle xenolith localities is summarised in Table 2 and typical hand specimen and thin section photographs are shown in Figure 4. Garnet is not present in mantle xenoliths of southern Victoria Land, though mantle clinopyroxene grains high in Na, relative to other mantle clinopyroxene grains from the same Mount Morning locality, have been interpreted as originating in the garnet stability field (Martin et al. 2015a). Plagioclase has been identified in some peridotite xenoliths. Amphibole is conspicuously absent from the Mount Morning Volcanic Field relative to all other southern Victoria Land mantle xenolith localities. Only a single phlogopite-bearing sample, from Mount Morning, has been reported. Glass is reported in several xenolith types from Foster Crater but is uncommon elsewhere in the province. Rare, texturally equilibrated carbonate and FeNi-sulphide grains have been

described in Mount Morning peridotite xenoliths and carbonate is present in a pyroxenite xenolith from Foster Crater.

The different peridotite rock types reflect different mantle processes. In a study of Mount Morning mantle xenoliths, Martin et al. (2015a) found spinel lherzolite made up 53% of the peridotite xenoliths collected, spinel harzburgite 35%, plagioclase-bearing spinel lherzolite 7% and spinel dunite 5%. These abundances are applicable across the wider province, where spinel lherzolite is the most common xenolith type, followed closely by spinel harzburgite (Kyle et al. 1987; Table 1; Table 2). Spinel dunite is uncommon relative to lherzolite or harzburgite but has been found at every significant xenolith locality (Table 2). Plagioclase-bearing spinel lherzolite (plagioclase lherzolite hereafter) is rare, and only reported at White Island, Mount Morning, and several Southern Local Suite locations, including Roaring Valley, Pipecleaner Glacier, The Bulwark and Foster Crater (Gamble et al. 1988; Moscati 1989; Cooper et al. 2007; Martin et al. 2014a).

Porphyroclastic describes a heterogranular metamorphic texture characterised by volumetrically significant amounts of both porphyroclasts and neoblasts. It reflects low-strain plastic deformation and dynamic recrystallisation relative to other mantle textures (Harte, 1977). In the Erebus Volcanic Province, the evidence to date suggests peridotite textures are typically porphyroclastic but become more tabular granuloblastic (i.e. strained) in the Mount Morning Volcanic Field than elsewhere. This could suggest that the most intense locale of rift-activity is located close to the Transantarctic Mountains beneath the Mount Morning Volcanic Field (e.g. Martin et al., 2015b). This hypothesis remains to be tested by more comprehensive fabric studies, including quantitative microstructural crystallographic preferred orientation work.

Porphyroclasts of olivine and orthopyroxene are common, the latter frequently showing kink banding or exsolution lamellae of clinopyroxene and containing trails of fluid inclusions. Clinopyroxene porphyroclasts are rare and smaller (c. 2 mm) than olivine, orthopyroxene or spinel porphyroclasts (≤ 4 mm). Orthopyroxene porphyroclasts are in places observed with exsolution

lamellae of secondary clinopyroxene. In some cases, spinel oikocrysts poikiloblastically enclose chadocrysts of clinopyroxene. Neoblasts of olivine, orthopyroxene and clinopyroxene are common (c. 0.5 mm in maximum dimension). Clinopyroxene neoblasts occur either in textural equilibrium with adjacent grains, or as late-stage growth along grain boundaries. Feldspar, when present, occurs only as neoblasts and is always found with spinel. Amphibole occurs as a common accessory mineral. Grains of carbonate, sulphide and apatite are rare and occur as neoblasts.

Pyroxenite xenoliths have been recorded in each volcanic field, but in all fields their abundance is low relative to the number of peridotite xenoliths, with one estimate putting the proportions at 80:20 peridotite:pyroxenite (Martin et al. 2015a). A full range of mineralogical variants is present, including wehrlite, olivine clinopyroxenite and clinopyroxenite of the Al-augite series and orthopyroxenite, websterite and olivine websterite of the Cr-diopside series. A rare rock type, glimmerite (phlogopite pyroxenite), is reported from Foster Crater (Gamble et al. 1988). Pyroxenite Cr-diopside series textures are equant or granuloblastic and pyroxenite Al-augite series textures are typically equigranular or coarsely porphyritic.

Mineral major element chemistry

Mantle peridotite ***olivine*** forsterite content varies between 81.8 and 91.9 %. On a plot of Ni/Fe versus Fo content (Fig. 5), olivine compositions from the Ross Island Volcanic Field mostly have lower forsterite contents, at a given Ni/Fe, relative to olivine grains from other volcanic fields in the province (Fig. 5a). This relationship is also true for olivine grains in pyroxenite xenoliths from the Erebus Volcanic Province (Fig. 5b).

Pyroxene wt. % Al_2O_3 varies inversely with MgO content in pyroxene from both peridotite (Fig. 6a, b) and pyroxenite (Fig. 6c, d) mantle xenoliths. From the available data, there is no systematic variation in pyroxene chemistry between different volcanic fields. Clinopyroxene compositions are predominantly diopside with some augite; orthopyroxene is almost exclusively enstatite (ESM1).

Spinel compositional data are available for mantle xenoliths from the Southern Local Suite, Mount Morning and Mount Discovery volcanic fields (Fig. 7a). On a Cr# [(100.Cr/(Cr+Al)] versus Mg# [100.Mg/(Mg + Fe^{2+})] diagram (Fig. 7a), all bar one spinel composition from peridotite xenoliths plot within the field typical of continental rifts. Four spinel data from pyroxenite xenoliths plot outside the field typical of continental rifts, with the remaining majority plotting within the field. The data from Mount Morning Volcanic Field covers a wide range of Mg# and Cr# values (Fig. 7a). The spinel data from the Mount Discovery Volcanic Field plot in a relatively tight group and can be clearly distinguished from the Southern Local Suite Volcanic Field data (Fig. 7a).

Feldspars in peridotite xenoliths from Mount Morning Volcanic Field are andesine in composition (Fig. 7b; anorthite $(An)_{38.4-41.1}$); those from the Mount Discovery Volcanic Field are labradorite and bytownite ($An_{62.6-78.9}$) and those from the Southern Local Suite Volcanic Field range in composition from andesine through labradorite to bytownite ($An_{31.9-72.3}$). Feldspars in pyroxenite xenoliths from locations in the Mount Morning Volcanic Field are andesine to the low end of labradorite (Fig. 7b; $An_{37.1-50.9}$).

Whole rock major element chemistry

On a whole rock Al/Si versus Mg/Si plot (Fig. 8), Erebus Volcanic Province mantle peridotite data are inversely correlated. This suggests variable depletion and (re-) enrichment relative to primitive mantle. The data overlap with melting modelled at 2 GPa or even greater depths (Fig. 8). The patterns on the element ratio plot (Fig. 8) are also seen on peridotite and pyroxenite whole rock wt. % MgO versus Al_2O_3 plots, where abundances are inversely correlated (Fig. 9a, b). This is related to increased melting, or higher degrees of refertilisation (Fig. 9a), as seen on Figure 8.

On a wt. % MgO versus Na_2O abundance plot (Fig. 9c), some whole rock peridotite xenolith compositions overlap with batch and fractional melt model trajectories. Other data for several samples, however, plot away from these model paths which may be an indication of major element

refertilisation (Fig. 9c). This is also seen when whole rock La/Sm is plotted against Na/Sm (Fig. 9d). The pyroxenite data show a weak, inverse relationship between wt. % MgO and Na_2O abundances (Fig. 9e).

The FeO contents of peridotite whole rock samples have been recalculated from the original analyses assuming all iron is Fe^{2+} on an anhydrous basis (ESM1). The majority of the peridotite samples have FeO < 9 wt. %, and, on a plot of FeO content versus MgO abundance (Fig. 9f), they lie on the melting grid of Walter (2003). Some samples from the province have FeO > 9 wt. % and these scatter away from the melting grid, which may indicate major element refertilisation (Fig. 9f). This pattern can also be seen when whole rock La/Sm versus Fe/Sm is plotted (Fig. 9g). On the wt. % FeO versus MgO abundance diagram, pyroxenite whole rock compositions are distributed in a series of arrays, each indicating a particular Mg# value (Fig. 9h). The two amphibolite samples reflect an Mg# of ~60, wehrlite and olivine clinopyroxenite samples have Mg# of ~80, whereas many clinopyroxenite, websterite and orthopyroxenite compositions have Mg# of ~90 (Fig. 9h).

Mineral and whole rock trace element chemistry and isotopic data

Trace element chemistry is available for clinopyroxene grains from mantle peridotite xenoliths and for whole rock samples of mantle peridotite xenoliths from each of the five volcanic fields. On primitive mantle normalised extended element plots (Fig. 10), clinopyroxene patterns are depleted in Ti and Pb relative to elements of similar compatibility. In general, large ion lithophile and high field strength elements are enriched, relative to depleted mid-ocean ridge mantle (Fig. 10). For the Mount Discovery Volcanic Field, whole rock trace element chemistry is available for only one plagioclase lherzolite sample, whereas analyses of spinel harzburgite have been reported for the other four volcanic fields (ESM1). On a primitive mantle normalised extended element plot, the whole rock pattern for the Mount Discovery Volcanic Field sample shows Pb enrichment relative to Ce and Nd (Fig. 10). Normalised whole rock trace element patterns for samples from all other

volcanic fields are characterised by depletions in Pb and Ti, relative to elements of similar compatibility; the patterns are comparable to those of clinopyroxene grains (Fig. 10).

Isotopic data for mantle xenoliths from southern Victoria Land are limited. Strontium, Nd and Pb isotope data are available for samples from Mount Morning (Martin et al. 2015a; n = 6), Sr and Nd isotope data for southern Victoria Land are presented in a figure in McGibbon (1991) and $^{87}Sr/^{86}Sr$ data from one sample from Southern Local Suite and five samples from Ross Island Volcanic Field are reported by Stuckless and Erickson (1976). The isotopic data for peridotite mantle xenoliths plot close to the HIMU (High-μ: enriched in ^{206}Pb and ^{208}Pb and relatively depleted in $^{87}Sr/^{86}Sr$) field in $^{87}Sr/^{86}Sr$ versus $^{143}Nd/^{144}Nd$ space (not shown), but radiogenic Pb is never as high as in end-member HIMU (Martin et al. 2015a). Pyroxenite mantle xenolith isotopic data can be modelled as a mixture between subcontinental lithospheric mantle (SCLM) and EMI (Enriched Mantle I: low $^{143}Nd/^{144}Nd$, low $^{87}Sr/^{86}Sr$ and high $^{207}Pb/^{206}Pb$ and $^{208}Pb/^{204}Pb$ at a given value of $^{206}Pb/^{204}Pb$) or EMII (Enriched mantle II: low $^{143}Nd/^{144}Nd$, high $^{87}Sr/^{86}Sr$ and high $^{207}Pb/^{206}Pb$ and $^{208}Pb/^{204}Pb$ at a given value of $^{206}Pb/^{204}Pb$). The mixing models replicate to a high degree the isotopic compositions of mantle xenoliths in the Erebus Volcanic Province (Martin et al. 2015a).

Discussion

Geothermobarometry

Using data for lower crustal xenoliths, Berg et al. (1989) calculated a geotherm for southern Victoria Land. A petrological geotherm was additionally calculated using mineral compositions from mantle peridotite xenoliths from Mount Morning (Martin et al. 2015a) and elsewhere in the province (Moscati, 1989). Martin et al. (2014a) recorded that the highest mantle temperatures were from those samples in southern Victoria Land most recently affected by refertilisation, which they attributed to entrapment of syn-rift melts in the lithosphere (Fig. 11). The superimposition of hot peridotite bodies on cold uppermost mantle has also been postulated for northern Victoria Land (Wörner & Zipfel 1996). This can be seen in Figure 11 (hollow diamonds) where plagioclase

lherzolites from Martin et al. (2014a) with pressures and temperatures plotting in the plagioclase mantle stability field are linked (thin dotted line) to relict minerals recording original pressures and temperatures that equilibrated in the spinel mantle stability field. This also explains the plagioclase lherzolite sample (labelled as a relict grain on Fig. 11) plotting in the spinel-bearing mantle stability field. See Martin et al. (2014a) for further discussion. In this study, geothermobarometry calculated for selected mantle xenolith samples (ESM 1) from each of the volcanic fields in southern Victoria Land is summarised in Figure 11. The calculations were made using the temperature-independent barometer of Putirka (2008) and a thermometer using equilibrated clinopyroxene grains with Mg# > 75 (Putirka 2008): these same equations were used by Martin et al. (2015a) allowing direct comparison. The geothermobarometry calculations used in Figure 11 are highlighted in the ESM1. The geothermometer of Brey and Kohler (1990) is also shown in the ESM1 material for comparison but is not used in plotting Figure 11. Most pressure and temperature estimates obtained on mantle xenoliths from each of the volcanic fields suggest that the geotherm reported by Berg et al. (1989) is correct and are consistent with previously published pressure-temperature estimates obtained from xenoliths (Fig. 11; Moscati 1989). Terror Rift Volcanic Field mantle xenolith samples have some of the highest pressures of 11.0 and 12.6 kbar and an average temperature of c. 1000 °C. The Ross Island and Mount Discovery volcanic field xenolith samples chosen for study give lower pressures (4.0 – 6.0 kbar) relative to the Terror Rift Volcanic Field samples, though a more extensive dataset may reveal extended ranges. The pressure-temperature data calculated here indicate that the southern Victoria Land geotherm is relevant to all volcanic fields in the province.

Mantle water content and oxygen fugacity

Water contents have not yet been directly estimated for southern Victoria Land mantle samples, so other lines of evidence must be considered. Iacovino et al. (2016) performed experiments on volcanic rocks from Ross Island Volcanic Field to show that there was c. 1-2 wt. % H_2O in magmas represented by the eruptives thought to be connected to their mantle source via a deep mafic

plumbing system. Studying olivine-hosted melt inclusions, Gaetani et al. (2019) suggested maximum wt. % H_2O was between 2.12 and 1.84 for the Ross Island Volcanic Field and the Mount Morning Volcanic Field. This would be consistent with volatile contents calculated for amphibole-bearing northern Victoria Land mantle of > 1 wt. % H_2O (Coltorti et al. this volume; Giacomoni et al. 2020). Though there are also relatively dry amphibole-free samples in north Victoria Land that only have wt. % H_2O < 0.4 (Perinelli et al. 2006). This suggests that, in general, the Victoria Land mantle is somewhat hydrous relative to, for example, the Antarctic Peninsula where water contents are c. 130 to 80 ppm (Gibson et al. 2020).

The mantle peridotite whole rock data plotted onto a parts per million (ppm) Yb versus V diagram, overlaps with the fields for oxygen fugacity relative to the fayalite-magnetite-quartz (FMQ) buffer calculated by Parkinson and Pearce (1998) between FMQ -0.5 and FMQ +1 (Fig. 12a). Specific localities have been studied further to refine oxygen fugacity estimates. At Mount Morning, oxygen fugacity calculated from Mössbauer spectroscopy measurements on spinel and pyroxene in mantle xenoliths showed a median value of -0.6 Δlog fO_2 relative to FMQ (Martin et al. 2015a). This is reduced relative to FMQ 1.3 to 1.8 Δlog fO_2 calculated from experiments for the deep plumbing system of primitive magma from the Ross Island Volcanic Field (Iacovino et al. 2016). Globally, Δlog fO_2 in rift settings varies between FMQ -4.1 to 0.5, with a median rift setting value of -0.9 ± 0.1 Δlog fO_2 (Frost and McCammon, 2008; Martin et al., 2015). In north Victoria Land, ΔLog fO_2 varies between -0.2 and -1.5 in anhydrous xenoliths and between -1.32 and -2.52 in amphibole-bearing (hydrous) xenoliths (Coltorti et al, this volume; Bonadiman et al., 2014; Perinelli et al., 2012). This shows the fO_2 values for the Erebus Volcanic Province overlap with the values typically expected within rift settings in Antarctica, and globally (Martin et al., 2015).

Origin of peridotite xenoliths

Melt depletion

Negative trends on wt. % MgO versus Al_2O_3 abundance plots for clinopyroxene (Fig. 6a), orthopyroxene (Fig. 6b) and whole rock data (Fig. 8, 9a) are commonly interpreted to reflect melt depletion in mantle xenoliths (e.g. Johnson et al. 1990; Niu 2004). Southern Victoria Land mantle clinopyroxene data plot adjacent to an equivalent melt trend and indicate up to 25% melting (Fig. 6a). The Mount Morning and Southern Local Suite volcanic fields have the most clinopyroxene data and these indicate a wide range of melt depletion values (1 - 25 %). There are fewer clinopyroxene data available for the three other volcanic fields and these indicate a more restricted range of melt depletion of between c. 10 and 25%. The plagioclase lherzolite data from Mount Morning and White Island are interpreted to show less melt depletion than is the case for spinel lherzolite or harzburgite xenoliths from the same localities. These comparisons also apply to the Mount Morning orthopyroxene in peridotite data (Fig. 6b).

Application of a model melting grid to wt. % FeO versus MgO abundance data for whole rock samples indicates that southern Victoria Land peridotites could be residues from the equivalent of 10 to 35% melting (Fig. 9f). This agrees with a simple melt model applied to a wt. % MgO versus Al_2O_3 abundance plot, which indicates up to 30% melt depletion (Fig. 9a). On both plots, spinel harzburgite and spinel dunite xenoliths can be argued to have undergone more melt depletion than spinel lherzolite or plagioclase lherzolite xenoliths. Similar melt depletion trends are derived when trace element data are compared with calculated models. For example, < 25% melting is suggested for a model applied to Yb versus V abundance data (Fig. 10a), 1 to > 25% melting is calculated for trends on a Yb (ppm) versus Dy/Yb diagram (Fig. 10b) or <5 to c. 20% melting as shown on a clinopyroxene mantle normalised Yb versus Y plot (Fig. 10c).

Melting was modelled in both the spinel and garnet stability fields of the mantle (Fig. 10b), assuming anhydrous conditions. All the southern Victoria Land compositions overlap with the spinel stability field model. Melting pressures modelled for peridotite whole rock wt. % MgO versus FeO abundance plot (Fig. 9f) indicate final melting pressures of 10 – 30 kbar, equivalent to the spinel facies or spinel-

garnet facies of the mantle. This is similar to the 2 GPa or greater pressures estimated from melting models on Figure 8. In summary, the mantle peridotite xenoliths of southern Victoria Land may have undergone up to c. 25% melt depletion in the spinel mantle facies.

Evidence for refertilisation

On a wt. % MgO versus Na_2O abundance plot, several whole rock mantle xenoliths from southern Victoria Land have compositions that can be explained by fractional or batch melt models (Fig. 9c). However, other samples have elevated wt. % Na_2O at a given MgO concentration, relative to the melt models (Fig. 9c), or elevated Na/Sm at a given La/Sm (Fig. 9d), consistent with major element refertilisation. This pattern is also observed on a whole rock wt. % MgO versus FeO abundance plot, with one sample from the Southern Local Suite, two samples from Mount Morning and several samples from the Ross Island Volcanic Field having elevated wt. % FeO relative to calculated melting grids (Fig. 9f). This can also be seen on a La/Sm versus Fe/Sm plot (Fig. 9g). Re-enrichment of Na and Fe in peridotite xenolith samples is decoupled and are not interpreted to form part of the same event. Similar FeO enrichments documented in abyssal peridotites have been attributed to olivine addition by melt migration through previously depleted mantle residues (e.g. Niu 1997; Rampone et al. 2008), which would be consistent with the olivine-rich spinel dunite assemblages of samples from the Ross Island Volcanic Field recording the most elevated FeO abundances (Fig. 9f). Another striking feature of Ross Island Volcanic Field mantle xenoliths is that olivine grains have lower Ni/Fe and lower forsterite contents than olivine grains from other volcanic fields in the province (Fig. 5). This is the case for olivine in both peridotite and pyroxenite xenoliths (Fig. 5a, b). Another notable feature is the high FeO content (11.19 wt. % average) of Ross Island Volcanic Field spinel lherzolite samples relative to spinel dunite xenoliths (10.35 wt. % FeO average). The Mg# is lower in spinel lherzolites (88.5 versus 89.4). These features distinguish mantle xenoliths of the Ross Island Volcanic Field from those of other volcanic fields in the province (Fig. 5).

The primitive mantle normalised rare earth element (REE) patterns of mantle clinopyroxene and whole rock peridotite xenoliths from southern Victoria Land are shown in Figures 13a and b. Total REE abundances are elevated relative to those of primitive mantle. Plotted for comparison are modelled melt depletion curves (Fig. 13b; black solid lines). The mid-REE and heavy-REE patterns of the peridotite xenoliths match reasonably well with the melt extraction models; however, the light-REE values are elevated above the modelled curves (Fig. 13b), which can be explained by light-REE refertilisation (e.g. Müntener et al. 2004; Martin et al. 2015a).

Sources of refertilisation

A unique volcanic lineage from the Ross Island Volcanic Field is the Enriched Iron Series (Kyle et al. 1992), which is distinguished by elevated whole rock FeO abundances relative to other volcanic rock series in the Erebus Volcanic Province (Martin et al. 2021). In the Ross Island Volcanic Field, elevated FeO abundances occur in rocks representing primitive magmas, in peridotite and pyroxenite xenoliths and in mantle olivine. High FeO concentrations in the mantle have been attributed to recycling of iron-rich crust (Kellogg et al. 1999; Sobolev et al. 2007), exchange of iron across the core-mantle boundary (Garnero 2000; Humayun et al. 2004) or primordial sources (Rubie et al. 2004). Martin et al. (2021) have hypothesised that an eclogitic component is more significant in the mantle beneath the Ross Island Volcanic Field, than is the case in the fields to the west. This would be consistent with recycling of iron-rich crust. Alternatively, some workers have suggested that a mantle plume is present beneath the Ross Island Volcanic Field (Kyle et al. 1992; Phillips et al. 2018), which would be more consistent with the core-mantle boundary model for excess FeO. We propose that both the source of the enriched-iron series magmas and mantle xenoliths with elevated FeO have been refertilised by similar melts. Further study of these samples could hold the key to differentiating between a recycled crust and mantle plume origin.

Martin et al. (2015a) have proposed up to 5 wt. % alkalic melt refertilisation in peridotite xenoliths from Mount Morning. The effect on REE behaviour of adding alkalic melt to a depleted mantle

source is modelled in Figure 13b (black dashed line). The REE data for southern Victoria Land whole rock mantle xenoliths can be explained by models in which depleted mantle is refertilised by the addition of ≤ 5 wt. % alkalic melt. Martin et al. (2014a) have also shown that the chemistry of clinopyroxene in plagioclase lherzolite xenoliths from the Mount Discovery, Mount Morning and Southern Local Suite volcanic fields is consistent with up to 6 wt. % addition to the mantle of a normal mid-ocean ridge basalt melt.

Metasomatism

Evidence for metasomatism in the mantle beneath southern Victoria Land includes the presence in peridotite xenoliths of grains of amphibole, phlogopite, carbonate and sulphide. Spinel mineral chemistry is also consistent with metasomatism in some mantle peridotites (Fig. 7a); as has been seen also in spinel grains in peridotite xenoliths from northern Victoria Land (Perinelli et al. 2008). Primitive mantle-normalised extended element patterns of clinopyroxene and most xenolith whole rock samples have negative Nb and Ti anomalies (Fig. 10) that are difficult to reconcile solely with melt depletion and refertilisation processes. An average primitive mantle-normalised trace element pattern for subducted sediment calculated by Plank and Langmuir (1998) is characterised by depletions in Ti and Nb relative to mafic melt and this Ti and Nb depletion is similar to those observed in southern Victoria Land peridotite specimens (Fig. 10). Lead enrichment is also seen in the subducted sediment average (Plank & Langmuir 1998), but this feature is rare in the normalised trace element patterns of southern Victoria Land peridotites. However, it is seen in the Mount Discovery Volcanic Field whole rock plagioclase lherzolite data (Fig. 10) and has been reported in whole rock mantle xenolith data from Mount Morning Volcanic Field (Martin et al. 2015a). To further examine the role of a sedimentary component, the southern Victoria Land whole rock data are plotted onto Nb/U versus Ce/Pb discrimination diagram (Fig. 14). A common interpretation of trends on this type of diagram is that whole rock Ce/Pb < 9 reflects a sedimentary component (e.g. White 2010). Mount Morning Volcanic Field data have the lowest Ce/Pb values in the province, i.e. ≤

the mantle array (Fig. 14), with many values equal to or less than bulk continental crust (Fig. 14). The trace element ratios (Fig. 14) have elsewhere been interpreted as reflecting fluid (with a sedimentary component) metasomatism and this is most obvious in data for the Mount Morning Volcanic Field (Fig. 14). A hint regarding the nature of this sedimentary component can be obtained from $^{87}Sr/^{86}Sr$ and $^{143}Nd/^{144}Nd$ isotope data (Fig. 15), which indicate that one of the Mount Morning spinel harzburgite xenolith compositions is on a mixing line with the EMI isotope end member. Mixing of c. 80% HIMU and c. 20% EMI isotopic compositions can generate the isotopic composition of this harzburgite specimen. End-member EM1 is commonly equated with lower continental crust, ancient pelagic sediment or delaminated subcontinental lithosphere (Hofmann 2004). Xenolith data from northern Victoria Land also plot along this modelled mixing line (e.g. Melchiorre et al. 2011; Perinelli et al. 2011; Fig. 15).

Rare carbonate neoblasts, weak Zr/Sm depletion relative to average subducted sediment (Fig. 10) and strong U/Th fractionation in the whole rock and clinopyroxene data (Fig. 10) for the Southern Local Suite, Mount Morning and Mount Discovery volcanic field data, can be interpreted to be related to carbonatite metasomatism (e.g. Yaxley et al. 1991; Pfänder et al. 2012; Ackerman et al. 2013). Martin et al. (2015a) calculated that some aspects of volcanic and peridotite xenolith whole rock trace element behaviour can be explained by ≤ 0.1 wt. % carbonatite addition to the Mount Morning mantle. Clinopyroxene and whole rock data from Ross Island and Terror Rift volcanic fields show little U/Th fractionation (Fig. 10), but studies of primitive volcanic rocks and mantle xenoliths at Franklin Island have suggested a possible carbonatite component in their source (Aviado et al. 2015; Doherty 2016).

Source characteristics and timing

On primitive mantle normalised extended element plots, trace element patterns for southern Victoria Land peridotite samples are comparable with those of SCLM or depleted mid-ocean ridge mantle (Fig. 10). Spinel harzburgite and spinel dunite samples have Sr and Nd isotopic compositions

similar to those of the HIMU mantle end member (Fig. 15), though the Pb isotope composition (whole rock $^{206}Pb/^{204}Pb$: 18.21 to 19.69; ESM1) is less radiogenic than HIMU *sensu stricto*. The peridotite isotopic compositions are comparable to those of primitive volcanic rocks from Victoria Land and the southwest Pacific [Diffuse Alkaline Magmatic Province (Finn et al. 2005) on Fig. 15, area defined by yellow field]. There is an ongoing debate in the literature whether isotopic and chemical source characteristics in Cenozoic DAMP volcanic rocks come exclusively from the asthenosphere or reflect a lithospheric contribution (Lanyon et al., 1993; Panter et al. 2006; Timm et al. 2009; Martin et al. 2015; Martin et al. 2021). One of the spinel lherzolite samples in this study is isotopically more similar to depleted mid-ocean ridge mantle (Fig. 15), and mantle source characteristics for southern Victoria Land have been explained in terms of mixing between depleted mid-ocean ridge mantle and HIMU (Cooper et al. 2007; Sims et al. 2008; Day et al. 2019). It is our favoured interpretation that there is a HIMU component in the lithospheric mantle that has mixed with a depleted mid-ocean ridge mantle component. We can not discount the presence of a HIMU component also in the asthenosphere. To this depleted, HIMU peridotite mantle, various components were added at various times, including sedimentary and carbonatite fractions, and there is also evidence for refertilisation by various other melts including normal mid-ocean ridge basalt and alkalic compositions, and, beneath the Ross Island Volcanic Field, an iron-rich melt.

A two-stage model lead age for volcanic rocks from Ross Island Volcanic Field yields a 1500 Ma isochron, which was interpreted by Sun and Hanson (1975) as the time at which chemical heterogeneity developed in the mantle source. This age agrees with Palaeoproterozoic aluminachron stabilisation ages determined for the southern Victoria Land mantle (Doherty et al. 2012, 2013), but contrasts with young (< 250 Ma) ages interpreted for Hut Point Peninsula mantle xenoliths from Re-Os isotopes (Day et al. 2019). Martin et al. (2021) favoured an ancient (> 0.5 Ga) age for *in situ* development of HIMU in the mantle source of Erebus Volcanic Province rocks. It is our favoured interpretation that the mantle stabilised during the Palaeoproterozoic, allowing *in situ* development of the HIMU isotopic signature (see van der Meer et al. 2017 for an example from

Zealandia). Melts were added, possibly at < 250 Ma beneath Hut Point Peninsula, and alkalic melts have been added since the onset of magmatism in the region at c. 25 Ma (Martin et al. 2010).

Origin of pyroxenite xenoliths

Pyroxenite xenoliths are reported from all volcanic fields in the province. Detailed pyroxenite xenolith studies have been undertaken at Foster Crater (Gamble & Kyle 1987; Gamble et al. 1988; McGibbon 1991) and Mount Morning (Martin et al. 2015a). McGibbon (1991) used whole-rock Rb-Sr isochrons to yield a 439.2 ± 14.5 Ma formation age on a clinopyroxenite xenolith from Foster Crater. Gamble et al. (1988) identified a number of processes that they believed had affected the pyroxenite assemblage at Foster Crater including potassium metasomatism, dynamic recrystallisation, melt generation and infiltration and oxidation. A carbonate grain has also been described in one clinopyroxenite from Foster Crater (Table 2). Martin et al. (2015a) concluded that Mount Morning pyroxenite xenoliths have formed from melts derived from, or modified by, fluids derived from subducted, eclogitic oceanic crust. North Victoria Land cumulates and pyroxenite xenoliths are discussed in detail, for example, by Wörner et al. (1993) and Perinelli et al. (2011).

The pyroxenite clinopyroxene data used in this study can be interpreted to suggest that the Al-augite series xenoliths (websterite and olivine websterite) are less fertile than the Cr-diopside series xenoliths (Fig. 6c). The spinel data obtained from pyroxenite xenoliths are consistent with a degree of metasomatism (Fig. 7a). Olivine grains from xenoliths of the Ross Island Volcanic Field have lower Ni/Fe abundances and Fo contents than is observed in olivine in pyroxenite or peridotite xenoliths from elsewhere in the region (Fig. 5). Isotopic data for several Southern Local Suite Volcanic Field xenoliths overlap with the field for the Diffuse Alkaline Magmatic Province, isotopic compositions of spinel harzburgite and spinel dunite from southern Victoria Land, and with the HIMU mantle field (Fig. 15). Several other Southern Local Suite Volcanic Field and Mount Morning Volcanic Field samples have high $^{87}Sr/^{86}Sr$ and low $^{143}Nd/^{144}Nd$ relative to other xenoliths (Fig. 15) and these have isotopic compositions on a mixing line with the EMII mantle end-member. A mixing model between

sub-continental lithospheric mantle and upper continental crust indicates that the high $^{87}Sr/^{86}Sr$ values may be explained by up to 20% mixing with a crustal component, and this is our preferred hypothesis.

The clinopyroxenite xenoliths with HIMU isotopic compositions are likely to be ancient (> 0.5 Ga) to allow *in situ* growth of the HIMU component in a manner similar to that envisioned for the peridotite xenoliths. At least some of the southern Victoria Land pyroxenite xenoliths formed in the Ordovician-Silurian (439.2 ± 14.5 Ma; McGibbon 1991). A sedimentary component (EMII), likely to have been derived from the upper continental crust, has influenced the chemistry of some pyroxenite xenoliths. We favour a hypothesis whereby pyroxenite xenoliths formed from fluids derived from (or modified by) a subducting slab, possibly with an eclogitic component. The variability in trace element and isotope chemistry may indicate that modification happened more than once.

Petrogenesis and regional variability

The cross-section drawn in Figure 16 for south Victoria Land and cross-sections drawn for north Victoria Land across the rift shoulder, for example by Wörner (1999), share a high degree of similarity suggesting commonality in processes along significant stretches of the West Antarctic Rift System. The lithospheric mantle beneath southern Victoria Land stabilised sometime in the Palaeoproterozoic, but since that time it has undergone a complex history of multiple melt depletions, refertilisation and metasomatic events (Fig. 16). There may also be pockets of younger (< 250 Ma) mantle beneath Hut Point Peninsula. In some mantle xenoliths, up to 25% melt extraction occurred in the spinel mantle facies. The HIMU component in the southern Victoria Land mantle must be ancient (> 0.5 Ga) to allow for *in situ* growth. All volcanic fields have undergone some degree of alkalic melt refertilisation, probably since at least 25 Ma, and this may be contributing to high heat flow in the province (Wörner & Zipfel 1996; Martin et al. 2014a). The plagioclase lherzolite samples show evidence of mixing of depleted mantle with up to 6 wt. % of a normal mid-ocean ridge

basalt component. In addition, the mantle beneath Ross Island Volcanic Field has been refertilised by an iron-rich melt that may also be responsible for the Hut Point Peninsula Enriched Iron Series volcanic lineage, emplaced at c. 1.3 Ma (Kyle 1981; Smellie & Martin 2021). We attribute this iron-rich mantle source to metasomatism by a fluid from (or modified by) a subducted slab. We suggest the regional variation in iron is real as it is recorded in mantle peridotite xenoliths, pyroxenite xenoliths and primitive magma compositions in the Ross Island Volcanic Field. A carbonatite mantle component is inferred to be present in the mantle beneath all volcanic fields, but a sedimentary component, which can be modelled as lower continental crust (EMI), is more significant in the Mount Morning Volcanic Field mantle. It cannot be discounted that the lower continental crust component variability is attributed to selective sampling or temporal variation. Water and oxygen fugacity may be up to c. 2 wt. % and -0.6 $\Delta\log fO_2$.

Cross-cutting the southern Victoria Land peridotite mantle are pyroxenite veins, which were probably emplaced at multiple times: one set has to be ancient (> 0.5 Ga), again to allow for *in situ* growth of the HIMU isotopic signature, and another occurred during the Ordovician-Silurian. The pyroxenite samples have undergone up to 25% melt depletion and at Foster Crater potassium metasomatism has also occurred. The data for olivine from pyroxenite xenoliths in the Ross Island Volcanic Field record the effects of an iron-rich fluid, which is also inferred to have affected the compositions of peridotites from the same locality. A sedimentary component can be identified in mantle samples from the Southern Local Suite Volcanic Field and Mount Morning Volcanic Field, and these compositions can be modelled by mixing of depleted mantle with up to 20% of an upper continental crust (EMII) component.

Summary & Conclusions

Mantle xenoliths from southern Victoria Land have been collected and analysed for over one hundred years. Key objectives of this chapter have been to provide a synthesis of the petrography of all xenolith samples collected and analysed over the decades (Table 2) and to collate and interpret

all the chemical data available (ESM 1). Spinel lherzolite and spinel harzburgite are the most common xenolith types, followed by spinel dunite. A rare type of plagioclase lherzolite is found in several localities. A wide range of pyroxenite xenolith types occur in each volcanic field. The peridotite and pyroxenite xenolith samples indicate that the geochemistry and petrogenetic evolution of the mantle beneath southern Victoria Land is complex and dynamic. The lithospheric mantle stabilised in the Palaeoproterozoic but subsequently these depleted peridotitic compositions have been modified by a sequence of further melt depletion and metasomatic (melt and/or fluid) enrichment events. An ancient (>0.5 Ga) depleted, HIMU *sensu stricto* mantle has undergone carbonatite metasomatism and multiple melt-depletion events. Ross Island Volcanic Field mantle has an iron-rich component relative to other areas in the province, and there may be a component of young (< 250 Ma) mantle beneath Hut Point Peninsula. This southern Victoria Land mantle is cross-cut by pyroxenite bodies emplaced probably at multiple times and the compositions of some pyroxenite xenoliths can be modelled to have been affected by an upper continental crust (EMII) component.

Despite such a long history of research, there is a limited amount of published age constraints, radiogenic isotope data or volatile data on the southern Victoria Land mantle samples, and consequently it is difficult to rigorously constrain the petrogenetic history. There is a complete absence of H_2O measurements on mantle xenoliths, despite the importance of this parameter to mantle viscosity calculations and melting models. Some localities, for example Mount Discovery, northern Beaufort Island and the Dailey Islands, have not been mapped in sufficient detail to exclude the possibility that mantle xenoliths may be present. Furthermore, in other areas, for example Minna Bluff, the mantle xenoliths collected have ultimately not been analysed. There are many localities yet to be visited, and many more mantle xenoliths to be documented and analysed. Thus mantle xenolith studies will continue to be an important research area in southern Victoria Land for decades to come.

Acknowledgements

We thank R.J. Moscati (U.S. Geological Survey) for providing material and discussion. We wish to thank G. Wörner and R.J. Mocscati for thorough reviews and W. van der Wal for editorial handling. Antarctica New Zealand and the United States Antarctic Programme are thanked for logistical support and JG thanks VUW Antarctic Research Centre for logistic support over many seasons.

Figure Captions

Figure 1 A locality diagram for mantle xenoliths of southern Victoria Land. **a**. The continent of Antarctica, divided geographically into East Antarctica and West Antarctica by the Transantarctic Mountains (thick black line). The location of panel b. is indicated by the red rectangle. McMurdo Volcanic Group rocks occur between Cape Adare in the north and Mount Early / Mount Sheridan in the south. **b**. Southern Victoria Land with alkalic igneous rocks of the Erebus Volcanic Province shown in black. Key mantle xenolith localities are shown (red circles) with numbers equating to line entries in Table 2. Major eruptive centre names are shown in blue. Details for localities 7-16 and localities 26-35 are shown in panels **c**. and **d**. DVDP: dry valleys drilling project.

Figure 2 A diagram showing the location of the five volcanic fields that make up the Erebus Volcanic Province (Martin et al. 2021; Smellie and Martin, 2021).

Figure 3 Examples of mantle xenoliths in the field. **a**. A large peridotite xenolith from Franklin Island. The hammer is c. 1 m long. Photo: R. J. Moscati. **b**. Mantle xenoliths in outcrop at Mount Morning, including a spinel lherzolite xenolith (beneath hand lens), a spinel harzburgite xenolith with a strong lineation fabric (bottom right), a clinopyroxene megacryst (upper right, black) and a wehrlite xenolith (middle). The hand lens is c. 6 cm long. Photo A. F. Cooper.

Figure 4 Typical petrographic features of mantle xenoliths from southern Victoria Land. Left panels in each pair of columns are hand specimen photographs with the maximum dimension of each hand specimen provided. The accompanying thin section photographs (right hand panels in

each pair of columns) are typical fields of view (4 mm across), taken under crossed-polarised light. Textures are: dunite = coarse; harzburgite = tabular granuloblastic; lherzolite = porphyroclastic.

Figure 5 Olivine mineral chemistry, Ni/Fe versus forsterite (Fo) content for **a**. peridotite xenoliths and **b**. pyroxenite xenoliths. The data plotting with the lowest Ni/Fe and Fo content are interpreted to reflect refertilisation. Legend abbreviations are as follows: D: spinel dunite; H: spinel harzburgite; Ls: spinel lherzolite; Lp: plagioclase lherzolite; W: wehrlite; Oc: olivine clinopyroxenite; C: clinopyroxenite; Wb: websterite; Ow: olivine websterite; M: mixed xenolith with multiple rock types; O: orthopyroxenite; Am: amphibolite.

Figure 6 Pyroxene major element mineral chemistry plotted on wt.% MgO – Al_2O_3 diagrams for **a**. clinopyroxene from peridotite xenoliths, **b**. orthopyroxene from peridotite xenoliths, **c**. clinopyroxene from pyroxenite xenoliths and **d**. orthopyroxene from pyroxenite xenoliths. Primitive mantle (PM) values for clinopyroxene (Cpx) and orthopyroxene (Opx) are from McDonough and Sun (1995) and the theoretical residual trends (solid lines labelled with % melt extraction) follow Upton et al. (2011) using equations from Workman and Hart (2005). The legend abbreviations are as in Figure 5. North Victoria Land data (black squares) after Pelorosso et al. (2016).

Figure 7 Spinel and feldspar mineral chemistry for southern Victoria Land mantle xenoliths. **a**. Spinel Mg# [100Mg/(Mg + Fe^{2+})] versus spinel Cr# [(100Cr/(Cr+Al)]. The field of spinel facies peridotite xenoliths from continental rift settings (dashed line) is from Martin et al. (2014b). Peridotite and pyroxenite data are shown here on the one figure. **b**. Feldspar mineral chemistry in peridotite and pyroxenite xenoliths. An: anorthite; Ab: albite; Or: orthoclase. The legend abbreviations are as in Figure 5.

Figure 8 A whole rock Al_2O_3/SiO_2 versus MgO/SiO_2 plot showing southern Victoria Land data relative to northern Victoria land (Coltorti et al. this volume) and Marie Byrd Land data (Handler et al. this volume). Melt extraction curves of Herzberg (2004) are also shown for 2 GPa melt depletion (dashed line) and 1 GPa (solid line) with indications of expected residual composition after 20% melt extraction. Black square is primitive mantle (McDonough and Sun, 1995). The legend abbreviations are as in Figure 5.

Figure 9 Whole rock wt. % Al_2O_3, Na_2O and FeO abundances plotted against MgO content for mantle xenolith samples from southern Victoria Land. **a**, **c** and **f** show data for peridotite and **b**, **e** and **h** for pyroxenites. Whole rock peridotite xenolith data for La/Sm versus Na/Sm (**d**) or Fe/Sm (**g**) are also shown for comparison. All iron was calculated as Fe^{2+} assuming anhydrous conditions. The melting residues in panels a. and c. were calculated assuming polybaric near-fractional melting between 25 and 15 kbar (black curved lines) or isobaric batch melting between 20 and 10 kbar (grey line) after Niu (1997). Primitive mantle (PM) values are from McDonough and Sun (1995). Whole rock Mg# are shown as dashed lines for comparison in panels **e**. and **f**. Panel e. shows the melting grid of Walter (2003) as a function of pressure (kbar) and batch melt extraction (%). Trends expected for refertilisation are indicated by arrows. The legend abbreviations are as in Figure 5.

Figure 10 Primitive mantle (McDonough and Sun 1995) normalised extended element plots for clinopyroxene (left column) and whole rock (right column) data. From left to right, the elements are arranged in order of decreasing incompatibility with respect to peridotitic residue. Note that data from plagioclase lherzolite were used for the Mount Discovery Volcanic Field and spinel harzburgite for other volcanic centres, reflecting the availability of data. The data represent individual analyses

from the ESM1 and are not amalgamated totals. Plotted for comparison are typical values for subcontinental lithospheric mantle (SCLM; McDonough 1990); depleted mid-ocean ridge basalt mantle (DMM; Workman & Hart 2005); normal mid-ocean ridge basalt (N-MORB; Gale et al. 2013); a high-μ pattern (sample M-11) from Mangaia, Austral Islands (HIMU; Woodhead 1996) and; average global subducted sediment (GLOSS; Plank & Langmuir 1998).

Figure 11 A temperature–pressure plot showing values calculated using pyroxene compositions in mantle xenoliths (ESM 1) from southern Victoria Land (Putirka 2008). Plotted for comparison are spinel peridotite xenolith data from Mount Morning (hollow circles; Martin et al. 2015a) and plagioclase lherzolite data from Pipecleaner Glacier, Mount Morning and White Island (hollow diamonds; Martin et al. 2014a). The mantle fields for plagioclase (Pl), spinel (Spl) and garnet (Grt) peridotite and the dry solidus follow Borghini et al. (2011). Geotherms for southern Victoria Land (SVL; Berg et al. 1989), northern Victoria Land (NVL; Perinelli et al. 2006) and an idealised dynamic rift (Chapman 1986) are shown for comparison. The legend abbreviations are as in Figure 5.

Figure 12 Whole rock vanadium (V) abundance (**a**) and Dy/Yb ratio (**b**) plotted against Yb content for southern Victoria Land mantle xenoliths. Clinopyroxene Yb vs Y normalised to primitive mantle (McDonough and Sun, 1995) are also shown (**c**). The model in **a**. shows predicted melt extraction paths (degree of melting in %) relative to the fayalite-magnetite-quartz (FMQ) oxygen fugacity buffer (Parkinson & Pearce 1998). In **b**., data are compared with a model for fractional melting of primitive mantle (PM; McDonough and Sun 1995) using the melting modes and partition coefficients of Johnson et al. (1990) for anhydrous garnet and spinel facies conditions. The percent melt fraction data are shown. The pyroxenite field (dashed line) is from this study (ESM1). In **c**., the

melt model shows between <5% and c. 20% melt extraction. See ESM1 for modelling details. The legend abbreviations are as in Figure 5.

Figure 13 Primitive mantle normalised rare earth element data (McDonough and Sun 1995) for: **a**. clinopyroxene and **b**. xenolith whole rock data. Samples are the same as used in Figure 8. Idealised melt extraction models are shown (thin black lines) for spinel facies peridotite calculated using the melting modes from Kinzler (1997) and element distribution coefficients from Liu et al. (2012) and Kelemen et al. (1995). Melt fractions (%) are shown in the boxes. A mixing model was also calculated between an initial peridotite composition (grey dashed line; sample OU78521) and host basalt (sample OU78540; Martin et al. 2013), using the mineral-melt coefficients of Ionov et al. (2002). The 5 wt. % melt proportion model is shown (circled number on black dashed line).

Figure 14 Niobium/U versus Pb/Ce diagrams for peridotite mantle xenoliths. Mantle array values of Nb/U (47 ± 10) and Ce/Pb (25 ± 5) are from Hoffman et al. (1986). Global peridotite data is from Pearson et al. (2003). OIB: ocean island basalt; BCC: bulk continental crust. The legend abbreviations are as in Figure 5.

Figure 15 A $^{143}Nd/^{144}Nd$ versus $^{87}Sr/^{86}Sr$ diagram for mantle xenoliths from southern Victoria Land. The Southern Local Suite data is after McGibbon (1991). North Victoria Land (NVL) data is after Melchiorre et al. (2011) and Perinelli et al. (2011). DMM: depleted mid-ocean ridge mantle; HIMU: high-μ; EMI: enriched mantle I; EMII: enriched mantle II; UCC: upper continental crust. Yellow field represents volcanic rock data (Martin et al. 2013) from the diffuse alkaline magmatic province (Finn et al. 2005) and the dashed field represents typical subcontinental lithospheric mantle values (Jourdan et al. 2007). Two melt models have been calculated and plotted for comparison. Melt

fractions (%) for both models are shown. The mixing curve (thick black line) between EMI and HIMU uses the equations of Faure (1986) and the compositions of Rolland et al. (2009), using EMI: ($^{87}Sr/^{86}Sr$) = 0.705, 513 ppm Sr; ($^{142}Nd/^{144}Nd$) = 0.5122, 33 ppm Nd; HIMU: ($^{87}Sr/^{86}Sr$) = 0.703, 120 ppm Sr; ($^{142}Nd/^{144}Nd$) = 0.51285, 6.5 ppm Nd. The mixing curve between subcontinental lithospheric mantle (SCLM) and UCC (thin black line) uses the values and equations in Jourdan et al. (2007), including SCLM: ($^{87}Sr/^{86}Sr$) = 0.7043, 50 ppm Sr; ($^{142}Nd/^{144}Nd$) = 0.51244, 2 ppm Nd; UCC: ($^{87}Sr/^{86}Sr$) = 0.73847, 159 ppm Sr; ($^{142}Nd/^{144}Nd$) = 0.511800, 26 ppm Nd. The legend abbreviations are as in Figure 5.

Figure 16 A schematic interpretive diagram, not to scale, showing structures and composition of the southern Victoria Land mantle. The proposed lithospheric mantle has evolved through mixing between depleted mantle and HIMU with varying degrees of carbonatite metasomatism and multiple melt extraction events. It is cross-cut by pyroxenite bodies, and the west is enriched in a sedimentary component relative to the east which has iron-rich melt. Plagioclase facies mantle is restricted to Mount Discovery Volcanic Field and further west. The crustal section of the cross-section follows seismic data interpretations made in Naish et al. (2007).

Tables

Table 1 Southern Victoria Land locations where mantle xenoliths have been recorded, including relevant references and rock types observed. The numbers (column labelled #) correspond to locations on figure 1.

Volcanic Field		Location	#	Reference(s)			Xenolith types
				1	2	3	
Terror Rift	Franklin Island	-	1	19	7	This Study	harzburgite, dunite, wehrlite
	Beaufort Island	-	-	-	-	-	Reconnaissance only. Further examination may show xenoliths
	submarine volcanic rocks	-	-	-	-	-	No xenoliths reported to date
Ross Island	Mount Bird	Cape Bird	2	3	-	-	clinopyroxenite
	Mount Terror	Conical Hill	3	7	This Study	-	harzburgite
		"Coastal Cliffs"	4	4	8	22	dunite, harzburgite, lherzolite, wehrlite
		The Knoll	5	19	7	This Study	lherzolite, harzburgite
	Mount Erebus	Summit area	-	-	-	-	Area examined but no xenoliths reported
		Dellbridge Islands	-	-	-	-	Area examined but no xenoliths reported
	Hut Point Peninsula	Turtle Rocks	6	19	7	This Study	dunite, wehrlite, clinopyroxenite
		"Sulphur Cones"	7	21	7	This Study	dunite, harzburgite, lherzolite
		Half Moon crater	8	22	12	-	harzburgite, lherzolite, wehrlite, clinopyroxenite
		"Ski Field"	9	21	12	-	dunite
		"McMurdo"	10	19	22	6	harzburgite, clinopyroxenite

		"North Twin Crater"	11	21	12	-	dunite
		Twin Crater	12	22	12	-	peridotite
		Crater Hill	13	8	21	12	dunite, peridotite
		"Eroded Volcanic Neck"	14	9	12	-	dunite, harzburgite, wehrlite
		Hut Point	15	19	21	12	dunite, clinopyroxenite
		DVDP	16	23	12	6	dunite
Mount Discovery	White Island	Mount Hayward and Camp Crater	17	5	14	7	dunite, harzburgite, lherzolite, pllherzolite, wehrlite, websterite, clinopyroxenite, pyroxene
	Black Island	-	18	3	12	-	peridotite, clinopyroxenite, wehrlite
	Minna Bluff	-	19	18	-	-	peridotite
	Mount Discovery	Discovery Saddle	20	12	-	-	dunite, wehrlite
	Brown Peninsula	-	-	11	-	-	Area examined but no xenoliths reported
	Dailey Islands	-	-	-	-	-	Reconnaissance only. Further examination may show xenoliths
Mount Morning	Mount Morning	Hurricane Ridge	21	13	15	-	dunite, harzburgite, lherzolite, wehrlite, clinopyroxenite
		Lake Morning	22	12	13	15	dunite, harzburgite, lherzolite, wehrlite, clinopyroxenite
		Riviera Ridge	23	13	15	7	dunite, harzburgite, lherzolite, pllherzolite, wehrlite, clinopyroxenite
	Mason Spur	Windscoop Bluff	24	12	13	15	dunite, harzburgite, lherzolite, wehrlite, clinopyroxenite
		Anniversary Bluff	25	12	13	15	dunite, harzburgite, lherzolite, wehrlite, clinopyroxenite
Southern Local Suite	Royal Society Range	Hooper Crags	26	20	12	-	dunite
		Foster Crater	27	24	10	7	dunite, clinopyroxenite, wehrlite, websterite, glimmerite
		Roaring Valley	28	25	12	17	dunite, peridotite, clinopyroxenite
		The Bulwark	29	2	12	17	harzburgite, lherzolite, pllherzolite

	Pipecleaner Glacier	30	25	14	7	lherzolite, pllherzolite, wehrlite
	Walcott Valley	31	25	12	-	peridotite
	Chancellor Lakes	32	26	12	-	peridotite, clinopyroxenite
	Heald Island	33	25	12	-	peridotite
	Brandau Crater	34	16	22	26	dunite, harzburgite, lherzolite, wehrlite, websterite, clinopyroxenite
	Howchin Glacier	35	12	-	-	lherzolite, wehrlite
Taylor Valley	-	-	1	-	-	Area examined but no xenoliths reported

1. (Allibone et al. 1991); 2.(Armstrong 1978); 3.(Cole & Ewart 1968); 4.(Cole et al. 1971); 5.(Cooper et al. 2007); 6.(Day et al. 2019); 7.(Doherty 2016); 8.(Ferrar 1907); 9.(Forbes & Banno 1966); 10.(Gamble et al. 1988); 11.(Kyle et al. 1979); 12.(Kyle et al. 1987); 13.(Martin 2009); 14.(Martin et al. 2014a); 15.(Martin et al. 2015a); 16.(McIver & Gevers 1970); 17.(Moscati 1989); 18.(Panter et al. 2011); 19.(Prior 1907); 20.(Skinner et al. 1976); 21.(Smith 1954); 22.(Stuckless & Ericksen 1976); 23.(Treves & Kyle 1973); 24.(Wright 1979a); 25.(Wright 1979b); 26.(Wright 1979c).

Table 2 Typical petrography of mantle xenoliths from southern Victoria Land.

Volcanic Field		Location	D	H	L		Ol	Cpx	Opx	Spl	Pl	Amp	Phl	Other	Texture	Size
Terror Rift	Franklin Island	-	Y	Y	Y		■	■	■	■		▒	▒	apatite		
Ross Island	Mount Bird				Y		■	■	■	■						
						peridot	■							Ol		
	Mount Terror		Y	Y	Y		■	■	■	■						
	Hut Point						■	■	■	■		▒				
	Peninsula		Y	Y	Y		■	■	■	■		▒				
						wehrlite	■	■								
						megacrysts	■	■						Ol + Cpx		
Mount Discovery	White Island		Y	Y	Y		■	■	■	■	▒	▒		anorthoclase megacrysts	protogranular	15-25 cm
						olivine	■	■								
						clinopyroxenite	■	■								rare
						olivine websterite	■	■				▒				vein 8 mm-wide
						wehrlite	■	■				▒				band 1.3 cm-wide
						pyroxene		■								
						kaersutite						■				
	Black Island	-		Y	Y		■	■	■	■						
						clinopyroxenite		■								
						wehrlite	■	■								
	Minna Bluff	-		Y	Y		■	■	■	■						
						kaersutite						■				

	Mount Discovery		Y			wehrlite						
Mount Morning	Mount Morning	-	Y	Y	Y			Cb		tabular granuloblastic	≤ 50 cm	
		-				orthopyroxenite				equant granuloblastic	≤ 30 cm	
						olivine websterite				equant granuloblastic	≤ 30 cm	
						websterite				equant granuloblastic	≤ 30 cm	
						wehrlite				equigranular	≤ 30 cm	
						clinopyroxenite				coarsely porphyritic	≤ 30 cm	
						clinopyroxene clinopyroxenite					5 cm	
	Mason Spur		Y	Y	Y	megacrysts				tabular granuloblastic	≤ 15 cm	
Southern Local Suite		Hooper Crags	Y									
		Roaring Valley		Y	Y					porphyroclastic	1 - 50 cm	
						clinopyroxenite megacrysts		Ol + Cpx				

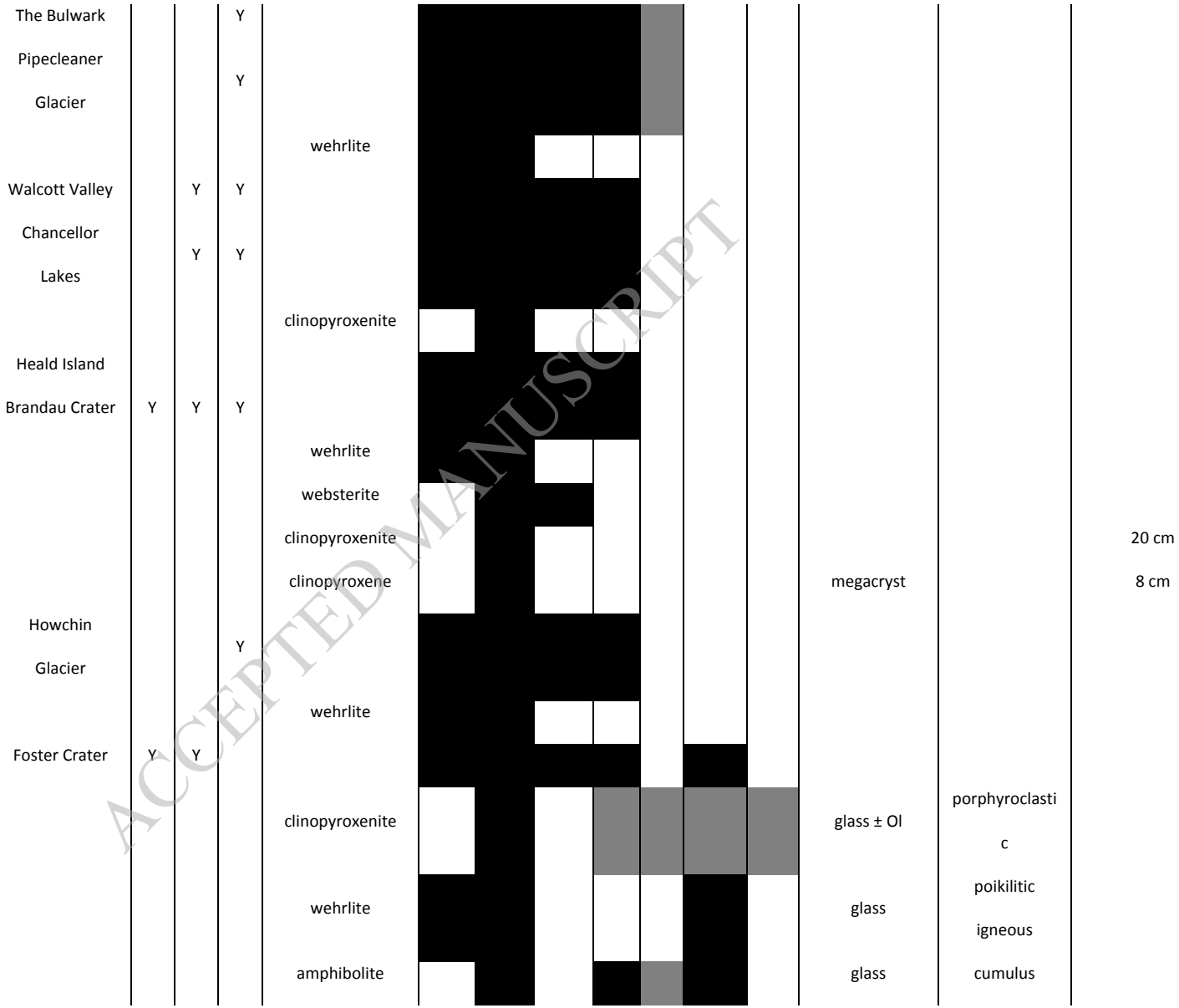

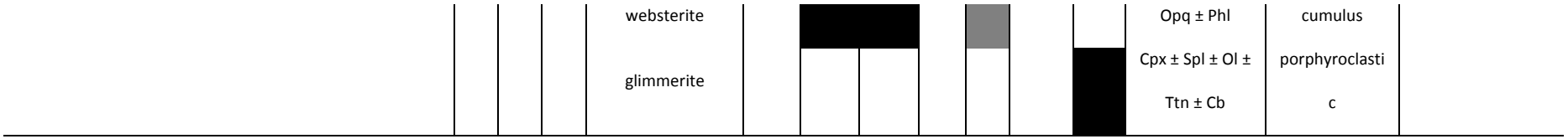

D: dunite; H: harzburgite; L: lherzolite; Ol: olivine: Cpx: clinopyroxene; Opx: orthopyroxene; Spl: spinel; Pl: plagioclase; Amp: amphibole; Phl: phlogopite; Ttn; titanite; Cb: carbonate. **Black** squares indicate dominant mineralogy and grey squares indicate minor mineralogy that is variably present.

References

Ackerman, L., ŠpaČek, P., Magna, T., Ulrych, J., Svojtka, M., Hegner, E. & Balogh, K. 2013. Alkaline and Carbonate-rich Melt Metasomatism and Melting of Subcontinental Lithospheric Mantle: Evidence from Mantle Xenoliths, NE Bavaria, Bohemian Massif. *Journal of Petrology*, **54**, 2597-2633, http://doi.org/10.1093/petrology/egt059.

Allibone, A.H., Forsyth, P.J., Sewell, R.J., Turnbull, I.M. & Bradshaw, M.A. 1991. *Geology of the Thudergut Area, southern Victoria Land, Antarctica 1:50 000*. New Zealand Geological Survey Micellaneous Geological Map 21, Wellington, New Zealand. Department of Scientific and Industrial Research.

Armstrong, R.L. 1978. K-Ar dating: Late Cenozoic McMurdo Volcanic Group and dry valley glacial history, Victoria Land, Antarctica. *New Zealand Journal of Geology and Geophysics*, **21**, 685-698, http://doi.org/10.1080/00288306.1978.10425199.

Aviado, K.B., Rilling- Hall, S., Bryce, J.G. & Mukasa, S.B. 2015. Submarine and subaerial lavas in the West Antarctic Rift System: Temporal record of shifting magma source components from the lithosphere and asthenosphere. *Geochemistry, Geophysics, Geosystems*, **16**, 4344-4361, http://doi.org/doi:10.1002/2015GC006076.

Barrett, P.J. 1981. History of the Ross Sea region during the deposition of the Beacon Supergroup 400-180 million years ago. *Journal of the Royal Society New Zealand*, **11**, 447 - 458.

Bédard, J.H.J., Marsh, B.D., Hersum, T.G., Naslund, H.R., Mukasa, S.B., 2007. Large-scale Mechanical Redistribution of Orthopyroxene and Plagioclase in the Basement Sill, Ferrar Dolerites, McMurdo Dry Valleys, Antarctica: Petrological, Mineral-chemical and Field Evidence for Channelized Movement of Crystals and Melt. *Journal of Petrology*, **48**, 2289-2326.

Berg, J.H., Moscati, R.J. & Herz, D.L. 1989. A petrologic geotherm from a continental rift in Antarctica. *Earth and Planetary Science Letters*, **93**, 98-108.

Borghini, G., Fumagalli, P. & Rampone, E. 2011. The geobarometric significance of plagioclase in mantle peridotites: A link between nature and experiments. *Lithos*, **126**, 42-53, http://doi.org/http://dx.doi.org/10.1016/j.lithos.2011.05.012.

Burgess, S.D., Bowring, S.A., Fleming, T.H. & Elliot, D.H. 2015. High-precision geochronology links the Ferrar large igneous province with early-Jurassic ocean anoxia and biotic crisis. *Earth and Planetary Science Letters*, **415**, 90-99, http://doi.org/http://dx.doi.org/10.1016/j.epsl.2015.01.037.

Chapman, D.S. 1986. Thermal gradients in the continental crust. *Geological Society, London, Special Publications*, **24**, 63-70, http://doi.org/10.1144/gsl.sp.1986.024.01.07.

Cole, J.W. & Ewart, A. 1968. Contributions to the volcanic geology of the Black Island, Brown Peninsula, and Cape Bird areas, McMurdo sound, Antarctica. *New Zealand Journal of Geology and Geophysics*, **11**, 793-828, http://doi.org/10.1080/00288306.1968.10420754.

Cole, J.W., Kyle, P.R. & Neall, V.E. 1971. Contributions to quaternary geology of Cape Crozier, White Island and Hut Point Peninsula, McMurdo Sound region, Antarctica. *New Zealand Journal of Geology and Geophysics*, **14**, 528-546, http://doi.org/10.1080/00288306.1971.10421946.

Cooper, A.F., Adam, L.J., Coulter, R.F., Eby, G.N. & McIntosh, W.C. 2007. Geology, geochronology and geochemistry of a basanitic volcano, White Island, Ross Sea, Antarctica. *Journal of Volcanology and Geothermal Research*, **165**, 189-216.

Cox, S.C., Turnbull, I.M., Isaac, M.J., Townsend, D.B. & Smith Lyttle, B. 2012. Geology of southern Victoria Land Antarctica. *Institute of Geological and Nuclear Sciences 1:250 000 Geological Map 22.*, **1 sheet + 135 p. Lower Hutt, New Zealand. GNS Science**.

Dannberg, J., Eilon, Z., Faul, U., Gassmöller, R., Moulik, P. & Myhill, R. 2017. The importance of grain size to mantle dynamics and seismological observations. *Geochemistry, Geophysics, Geosystems*, **18**, 3034-3061, http://doi.org/10.1002/2017gc006944.

Davis, F.A., Tangeman, J.A., Tenner, T.J. & Hirschmann, M.M. 2009. The composition of KLB-1 peridotite. *American Mineralogist*, **94**, 176-180.

Day, J.M.D., Harvey, R.P. & Hilton, D.R. 2019. Melt-modified lithosphere beneath Ross Island and its role in the tectono-magmatic evolution of the West Antarctic Rift System. *Chemical Geology*, **518**, 45-54, http://doi.org/https://doi.org/10.1016/j.chemgeo.2019.04.012.

Doherty, C., Class, C., Goldstein, S.L., Shirey, S.B., Martin, A.P., Cooper, A.F., Berg, J.H. & Gamble, J.A. 2012. Constraining the dynamic response of subcontinental lithospheric mantle to rifting using Re-Os model ages in the Western Ross Sea, Antarctica. Abstract presented at 2012 Fall Meeting. *AGU*, San Francisco, California.

Doherty, C., Class, C., Goldstein, S.L., Shirey, S.B., Martin, A.P., Cooper, A.F., Berg, J.H. & Gamble, J.A. 2013. Re-Os systematics of the lithospheric mantle beneath the Western Ross Sea area, Antarctica: depletion ages and dynamic response during rifting *AGU*, San Francisco, 9-13 December, T13A-2516.

Doherty, C.L. 2016. *Multi-stage evolution of the lithospheric mantle in the West Antarctic Rift System-a mantle xenolith study.* Ph.D, Columbia University.

Eggins, S.M., Woodhead, J.D., Kinsley, L., Mortimer, G., Sylvester, P., McCulloch, M.T., Hergt, J.M., and Handler, M., 1997: A simple method for the precise analysis of 40 or more trace elements in geological materials by ICPMS using enriched isotope internal standardization. Chemical Geology, 134, 311- 326.
Faure, G. 1986. *Principles of isotope geology, 2nd edition*. Wiley, New York.

Ferrar, H.T. 1907. Report on the field-geology of the region explored during the "Discovery" Antarctic expedition, 1901 - 1904. *Natural History*, **1**, 1-100.

Fielding, C.R., Henrys, S.A. & Wilson, T.J. 2006. Rift history of the western Victoria Land Basin: a new perspective based on integration of cores with seismic reflection data. *In*: Futterer, D.K., Damaske, D., Kleinschmidt, G., Miller, H. & Tessensohn, F. (eds) *Antarctica: Contributions to Global Earth Sciences*. Springer-Verlag, Berlin, 307-316.

Finn, C.A., Müller, R.D. & Panter, K.S. 2005. A Cenozoic diffuse alkaline magmatic province (DAMP) in the southwest Pacific without rift or plume origin. *Geochemistry, Geophysics, Geosystems*, **6**, Q02005, http://doi.org/10.1029/2004gc000723.

Fitzgerald, P. 2002. Tectonics and landscape evolution of the Antarctic plate since the breakup of Gondwana, with an emphasis on the West Antarctic Rift System and the Transantarctic Mountains. *Royal Society of New Zealand Bulletin*, **35**, 453-469.

Forbes, R.B. 1963. Ultrabasic inclusion from the basalts of the Hut Point area, Ross Island, Antarctica. *Bulletin Volcanologique*, **26**, 13-21, http://doi.org/10.1007/BF02597270.

Forbes, R.B. & Banno, S. 1966. Nickel-iron content of peridotite inclusion and cognate olivine from an Alkali-Olivine Basalt. *American Mineralogist*, **51**, 130-140.

Gale, A., Dalton, C.A., Langmuir, C.H., Su, Y. & Schilling, J.-G. 2013. The mean composition of ocean ridge basalts. *Geochemistry, Geophysics, Geosystems*, **14**, 489-518, http://doi.org/10.1029/2012gc004334.

Gamble, J.A. & Kyle, P.R. 1987. The origins of glass and amphibole in spinel-wehrlite xenoliths from Foster Crater, McMurdo Volcanic Group, Antarctica. *Journal of Petrology*, **28**, 755-779.

Gamble, J.A., McGibbon, F., Kyle, P.R., Menzies, M. & Kirsch, I. 1988. Metasomatised xenoliths from Foster Crater, Antarctica: Implications for lithospheric structure and process beneath the Transantarctic Mountain front. *Journal of Petrology*, **Special Volume 1**, 109-138, http://doi.org/10.1093/petrology/Special_Volume.1.109.

Garnero, E.J. 2000. Heterogeneity of the lowermost mantle. *Annual Review of Earth and Planetary Sciences*, **28**, 509-537.

Green, D.H. & Falloon, T.J. 1998. *Pyrolite: A Ringwood Concept and Its Current Expression*. Cambridge University Press.

Gunn, B.M. & Warren, G. 1962. Geology of Victoria Land between the Mawson and Mullock Glaciers, Antarctica. *Bulletin of the New Zealand Geological Survey*, **71**, 157.

Hall, J., Wilson, T., Henrys, S., Cooper, A. & Raymond, C. 2007. Structure of the central Terror Rift, western Ross sea, Antarctica. *Antarctica: A Keystone in a Changing World—Online Proceedings of the 10th ISAES: USGS Open-File Report*, **1047**.

Harrington, H.J. 1958. Nomenclature of rock units in the Ross Sea Region, Antarctica. *Nature*, **182**, 290.

Hofmann, A.W. 2004. Sampling mantle heterogeneity through oceanic basalts; isotopes and trace elements. *In*: Carlson, R.W., Holland, H.D. & Turekian, K.K. (eds) *The Mantle and Core, volume 2*. Elsevier, Oxford, 61-102.

Hofmann, A.W., Jochum, K.P., Seufert, M., White, W.M., 1986. Nb and Pb in oceanic basalts: new constraints on mantle evolution. *Earth and Planetary Science Letters*, **79**, 33-45.
Humayun, M., Qin, L. & Norman, M.D. 2004. Geochemical Evidence for Excess Iron in the Mantle Beneath Hawaii. *Science*, **306**, 91, http://doi.org/10.1126/science.1101050.

Iacovino, K., Oppenheimer, C., Scaillet, B. & Kyle, P. 2016. Storage and evolution of mafic and intermediate alkaline magmas beneath Ross Island, Antarctica. *Journal of Petrology*, **57**, 93-118.

Ionov, D.A., Bodinier, J.-L., Mukasa, S.B. & Zanetti, A. 2002. Mechanisms and Sources of Mantle Metasomatism: Major and Trace Element Compositions of Peridotite Xenoliths from Spitsbergen in the Context of Numerical Modelling. *Journal of Petrology*, **43**, 2219-2259.

Jaques, A. & Green, D. 1980. Anhydrous melting of peridotite at 0–15 kb pressure and the genesis of tholeiitic basalts. *Contributions to Mineralogy and Petrology*, **73**, 287-310.

Johnson, K.T.M., Dick, H.J.B. & Shimizu, N. 1990. Melting in the oceanic upper mantle: An ion microprobe study of diopsides in abyssal peridotites. *Journal of Geophysical Research: Solid Earth*, **95**, 2661-2678, http://doi.org/10.1029/JB095iB03p02661.

Jourdan, F., Bertrand, H., Schärer, U., Blichert-Toft, J., Féraud, G. & Kampunzu, A.B. 2007. Major and Trace Element and Sr, Nd, Hf, and Pb Isotope Compositions of the Karoo Large Igneous Province, Botswana–Zimbabwe: Lithosphere vs Mantle Plume Contribution. *Journal of Petrology*, **48**, 1043-1077.

Kelemen, P.B., Shimizu, N. & Salters, V.J.M. 1995. Extraction of mid-ocean-ridge basalt from the upwelling mantle by focused flow of melt in dunite channels. *Nature*, **375**, 747-753.

Kellogg, L.H., Hager, B.H. & Van Der Hilst, R.D. 1999. Compositional stratification in the deep mantle. *Science*, **283**, 1881-1884.

Kinzler, R.J. 1997. Melting of mantle peridotite at pressures approaching the spinel to garnet transition: Application to mid-ocean ridge basalt petrogenesis. *Journal of Geophysical Research: Solid Earth*, **102**, 853-874, http://doi.org/10.1029/96jb00988.

Kyle, P.R. 1981. Mineralogy and Geochemistry of a Basanite to Phonolite Sequence at Hut Point Peninsula, Antarctica, based on Core from Dry Valley Drilling Project Drillholes 1, 2 and 3. *Journal of Petrology*, **22**, 451-500, http://doi.org/10.1093/petrology/22.4.451.

Kyle, P.R. 1990. McMurdo Volcanic Group - western Ross Embayment: Introduction. *In*: LeMasurier, W.E. & Thompson, J. (eds) *Volcanoes of the Antarctic plate and southern oceans*, Antarctic Research Series 48:18-25.

Kyle, P.R., Adams, J. & Rankin, P.C. 1979. Geology and petrology of the McMurdo Volcanic Group at Rainbow Ridge, Brown Peninsula, Antarctica. *Geological Society of America Bulletin*, **90**, 676.

Kyle, P.R., Wright, A.C. & Kirsch, I. 1987. Ultramafic xenoliths in the late Cenozoic McMurdo Volcanic Group, western Ross Sea embayment, Antarctica. *In*: Nixon, P.H. (ed) *Mantle xenoliths*. John Wiley & Sons Ltd, Great Britain, 287-293.

Kyle, P.R., Moore, J.A. & Thirlwall, M.F. 1992. Petrologic Evolution of Anorthoclase Phonolite Lavas at Mount Erebus, Ross Island, Antarctica. *Journal of Petrology*, **33**, 849-875, http://doi.org/10.1093/petrology/33.4.849.

Lallemant, H.A., Mercier, J.C., Carter, N. & Ross, J. 1980. Rheology of the upper mantle: inferences from peridotite xenoliths. *Tectonophysics*, **70**, 85-113.

Lanyon, R., Varne, R., Crawford, A.J., 1993. Tasmanian Tertiary basalts, the Balleny plume, and opening of the Tasman Sea (southwest Pacific Ocean). *Geology*, **21**, 555-558.
Liu, J., Carlson, R.W., Rudnick, R.L., Walker, R.J., Gao, S. & Wu, F. 2012. Comparative Sr–Nd–Hf–Os–Pb isotope systematics of xenolithic peridotites from Yangyuan, North China Craton: Additional evidence for a Paleoproterozoic age. *Chemical Geology*, **332**, 1-14.

Martin, A.P. 2009. *Mount Morning, Antarctica: Geochemistry, geochronology, petrology, volcanology, and oxygen fugacity of the rifted Antarctic lithosphere.* Ph.D. thesis, University of Otago.

Martin, A.P. & Cooper, A.F. 2010. Post 3.9 Ma fault activity within the West Antarctic rift system: onshore evidence from Gandalf Ridge, Mount Morning eruptive centre, southern Victoria Land, Antarctica. *Antarctic Science*, **22**, 513-521, http://doi.org/doi:10.1017/S095410201000026X.

Martin, A.P., Cooper, A.F. & Dunlap, W.J. 2010. Geochronology of Mount Morning, Antarctica: Two-phase evolution of a long-lived trachyte-basanite-phonolite eruptive center. *Bulletin of Volcanology*, **72**, 357-371, http://doi.org/doi: 10.1007/s00445-009-0319-1.

Martin, A.P., Cooper, A.F. & Price, R.C. 2013. Petrogenesis of Cenozoic, alkalic volcanic lineages at Mount Morning, West Antarctica and their entrained lithospheric mantle xenoliths: Lithospheric versus asthenospheric mantle sources. *Geochimica et Cosmochimica Acta*, **122**, 127-152, http://doi.org/http://dx.doi.org/10.1016/j.gca.2013.08.025.

Martin, A.P., Cooper, A.F. & Price, R.C. 2014a. Increased mantle heat flow with on-going rifting of the West Antarctic rift system inferred from characterisation of plagioclase peridotite in the shallow Antarctic mantle. *Lithos*, **190-191**, 173-190.

Martin, A.P., Price, R.C. & Cooper, A.F. 2014b. Constraints on the composition, source and petrogenesis of plagioclase-bearing mantle peridotite. *Earth-Science Reviews*, **138**, 89-101, http://doi.org/http://dx.doi.org/10.1016/j.earscirev.2014.08.006.

Martin, A.P., Price, R.C., Cooper, A.F. & McCammon, C.A. 2015a. Petrogenesis of the Rifted Southern Victoria Land Lithospheric Mantle, Antarctica, Inferred from Petrography, Geochemistry, Thermobarometry and Oxybarometry of Peridotite and Pyroxenite Xenoliths from the Mount Morning Eruptive Centre. *Journal of Petrology*, **56**, 193-226, http://doi.org/10.1093/petrology/egu075.

Martin, A.P., Cooper, A.F., Price, R.C., Turnbull, R.E. & Roberts, N.M.W. 2015b. The petrology, geochronology and significance of Granite Harbour Intrusive Complex xenoliths and outcrop sampled in western McMurdo Sound, Southern Victoria Land, Antarctica. *New Zealand Journal of Geology and Geophysics*, **58**, 33-51, http://doi.org/10.1080/00288306.2014.982660.

Martin, A.P., Cooper, A.F., Price, R.C., P.R., K. & Gamble, J.A. 2021. Erebus Volcanic Province II. Petrology. *In*: Smellie, J.L., Panter, K.S. & Geyer, A. (eds) *Volcanism in Antarctica: 200 Million Years of Subduction, Rifting and Continental Break-Up*. Geological Society, London.

McDonough, W.F. 1990. Constraints on the composition of the continental lithospheric mantle. *Earth and Planetary Science Letters*, **101**, 1-18.

McDonough, W.F. & Sun, S.-S. 1995. The composition of the Earth. *Chemical Geology*, **120**, 223-253.

McGibbon, F.M. 1991. Geochemistry and petrology of ultramafic xenoliths of the Erebus Volcanic Province. *In*: Thomson, M.R.A., Crame, J.A. & Thomson, J.W. (eds) *Geological evolution of Antarctica - Proceedings of the 5th International Symposium on Antarctic Earth Sciences*. Cambridge University Press, Cambridge, 317-321.

McGinnis, L.D., Bowen, R.H., Erickson, J.M., Alfred, B.J. & Kreamer, J.L. 1985. East-West Antarctic boundary in McMurdo Sound. *Tectonophysics*, **114**, 341-356.

McIver, J.R. & Gevers, T.W. 1970. Volcanic vents below the Royal Society Range, Central Victoria Land, Antarctica. *Transactions of the Geological Society of South Africa*, **73**, 65-88.

Melchiorre, M., Coltorti, M., Bonadiman, C., Faccini, B., O'Reilly, S.Y. & Pearson, N.J. 2011. The role of eclogite in the rift-related metasomatism and Cenozoic magmatism of Northern Victoria Land, Antarctica. *Lithos*, **124**, 319-330, http://doi.org/http://dx.doi.org/10.1016/j.lithos.2010.11.012.

Mercier, J.-C.C., Anderson, D.A. & Carter, N.L. 1977. Stress in the lithosphere: inferences from steady state flow of rocks *Stress in the Earth*. Springer, 199-226.

Moscati, R.J. 1989. *Petrology and thermobarometry of pyroxene granulite and spinel lherzolite xenoliths from a modern continental rift, Royal Society Range, McMurdo Sound region, Antarctica.* MSc, Northern Illinois University.

Müntener, O., Pettke, T., Desmurs, L., Meier, M. & Schaltegger, U. 2004. Refertilization of mantle peridotite in embryonic ocean basins: Trace element and Nd isotopic evidence and implications for crust-mantle relationships. *Earth and Planetary Science Letters*, **221**, 293-308.

Mysen, B.O. & Kushiro, I. 1977. Compositional variations of coexisting phases with degree of melting of peridotite in the upper mantle. *American Mineralogist*, **62**, 843-856.

Naish, T., Powell, R., Levy, R., Team, T.A.-M.S., 2007. Background to the ANDRILL McMurdo Ice Shelf Project (Antarctica) and Initial Science Volume. Terra Antarctica, 14: 121-130.

Niida, K. 1988. Metasomatic veins and minerals in mantle-derived xenoliths, Antarctica. *Proceedings of the NIPR Symposium on Antarctic Geoscience*, 67-69.

Niida, K. 1990. Glass in mantle-derived peridotite xenoliths from the McMurdo Volcanic Group, Antarctica. *Proceedings of the NIPR Symposium on Antarctic Geosciences*, 172-180.

Niu, Y. 1997. Mantle melting and melt extraction processes beneath ocean ridges: evidence from abyssal peridotites. *Journal of Petrology*, **38**, 1047-1074.

Niu, Y. 2004. Bulk-rock major and trace element compositions of abyssal peridotites: Implications for mantle melting, melt extraction and post-melting processes beneath mid-ocean ridges. *Journal of Petrology*, **45**, 2423-2458.

Palmer, K., 1990: XRF analyses of granitoids and associated rocks, St John's Range, South Victoria Land, Antarctica. Analytical Contribution 13, Victoria University, Antarctic Data Series, 15, 23pp.

Panter, K.S., Blusztajn, J., Hart, S.R., Kyle, P.R., Esser, R., McIntosh, W.C., 2006. The Origin of HIMU in the SW Pacific: Evidence from Intraplate Volcanism in Southern New Zealand and Subantarctic Islands. *Journal of Petrology*, **47**, 1673-1704.

Panter, K., Dunbar, N.W., Scanlan, M., Wilch, T., Fargo, A. & McIntosh, W. 2011. Petrogenesis of alkaline magmas at Minna Bluff, Antarctica: evidence for multi-stage differentiation and complex mixing processes: Abstract presented at 2011 Fall Meeting. *AGU*, San Francisco, California, v. V31F-2590.

Panter, K.S. 2021. Mt Early & Sheridan Bluff II. Petrology. *In*: Smellie, J.l., Panter, K.S. & Geyer, A. (eds) *Volcanism in Antarctica: 200 million years of subduction, rifting and continental break-up*. Geological Society, London.

Parkinson, I.J. & Pearce, J.A. 1998. Peridotites from the Izu–Bonin–Mariana Forearc (ODP Leg 125): Evidence for Mantle Melting and Melt–Mantle Interaction in a Supra-Subduction Zone Setting. *Journal of Petrology*, **39**, 1577-1618, http://doi.org/10.1093/petroj/39.9.1577.

Perinelli, C., Armienti, P. & Dallai, L. 2006. Geochemical and O-isotope constraints on the evolution of lithospheric mantle in the Ross Sea rift area (Antarctica). *Contributions to Mineralogy and Petrology*, **151**, 245-266, http://doi.org/10.1007/s00410-006-0065-8.

Perinelli, C., Armienti, P. & Dallai, L. 2011. Thermal Evolution of the Lithosphere in a Rift Environment as Inferred from the Geochemistry of Mantle Cumulates, Northern Victoria Land, Antarctica. *Journal of Petrology*, **52**, 665-690, http://doi.org/10.1093/petrology/egq099.

Perinelli, C., Orlando, A., Conte, A.M., Armienti, P., Borrini, D., Faccini, B. & Misiti, V. 2008. Metasomatism induced by alkaline magma in the upper mantle of northern Victoria Land (Antarctica): an experimental approach. *Geological Society, London, Special Publications*, **293**, 279-302, http://doi.org/10.1144/sp293.13.

Pfänder, J.A., Jung, S., Münker, C., Stracke, A. & Mezger, K. 2012. A possible high Nb/Ta reservoir in the continental lithospheric mantle and consequences on the global Nb budget – Evidence from continental basalts from Central Germany. *Geochimica et Cosmochimica Acta*, **77**, 232-251, http://doi.org/http://dx.doi.org/10.1016/j.gca.2011.11.017.

Phillips, E.H., Sims, K.W.W., Blichert-Toft, J., Aster, R.C., Gaetani, G.A., Kyle, P.R., Wallace, P.J. & Rasmussen, D.J. 2018. The nature and evolution of mantle upwelling at Ross Island, Antarctica, with implications for the source of HIMU lavas. *Earth and Planetary Science Letters*, **498**, 38-53, http://doi.org/https://doi.org/10.1016/j.epsl.2018.05.049.

Plank, T. & Langmuir, C.H. 1998. The chemical composition of subducting sediment and its consequence for the crust and mantle. *Chemical Geology*, **145**, 325-394.

Prior, G.T. 1902. Report on the rock specimens collected by the Southern Cross Antarctic Expedition, British Museum.

Prior, G.T. 1907. Report on the rock specimens collected during the "Discovery" Antarctic Expedition, 1901 - 1904. *Natural History*, **1**, 101-160.

Putirka, K.D. 2008. Thermometers and Barometers for Volcanic Systems. *Reviews in Mineralogy and Geochemistry*, **69**, 61-120, http://doi.org/10.2138/rmg.2008.69.3.

Rampone, E., Piccardo, G.B. & Hofmann, A.W. 2008. Multi-stage melt–rock interaction in the Mt. Maggiore (Corsica, France) ophiolitic peridotites: Microstructural and geochemical evidence. *Contributions to Mineralogy and Petrology*, **156**, 453-475.

Ringwood, A.E. 1962. A model for the upper mantle. *Journal of Geophysical Research (1896-1977)*, **67**, 857-867, http://doi.org/10.1029/JZ067i002p00857.

Rolland, Y., Galoyan, G., Bosch, D., Sosson, M., Corsini, M., Fornari, M. & Verati, C. 2009. Jurassic back-arc and Cretaceous hot-spot series In the Armenian ophiolites — Implications for the obduction process. *Lithos*, **112**, 163-187, http://doi.org/http://dx.doi.org/10.1016/j.lithos.2009.02.006.

Rubie, D.C., Gessmann, C.K. & Frost, D.J. 2004. Partitioning of oxygen during core formation on the Earth and Mars. *Nature*, **429**, 58-61, http://doi.org/10.1038/nature02473.

Siddoway, C. 2008. Tectonics of the West Antarctic rift system: New light on the history and dynamics of distributed intracontinental extension (invited paper). *In*: Cooper, I.K., Barrett, P., Stagg, H., Storey, B., Stump, E. & Wise, W. (eds) *Antarctica: A Keystone in a Changing World*. National Academy of Sciences, Washington, D.C., 91-114.

Sims, K.W.W., Blichert-Toft, J., Kyle, P.R., Pichat, S., Gauthier, P.-J., Blusztajn, J., Kelly, P., Ball, L.*, et al.* 2008. A Sr, Nd, Hf, and Pb isotope perspective on the genesis and long-term evolution of alkaline magmas from Erebus volcano, Antarctica. *Journal of Volcanology and Geothermal Research*, **177**, 606-618, http://doi.org/http://dx.doi.org/10.1016/j.jvolgeores.2007.08.006.

Skinner, D.N.B., Waterhouse, B.C., Brehaut, G.M. & Sullivan, K. 1976. New Zealand Geological Survey Antarctic Expedition 1975-76, Skelton-Koettlitz glaciers, Report DS58. *New Zealand Geological Survey*.

Smellie, J.L. & Martin, A.P. 2021. Southern Victoria Land. I. Volcanology. *In*: Smellie, J.L., Panter, K.S. & Geyer, A. (eds) *Volcanism in Antarctica: 200 million years of subduction, rifting and continental break-up*. Geological Society, London, Memoir.

Smith, W.C. 1954. *The volcanic rocks of the Ross archipelago, British Terra Nova Expedition, 1910. Natural History Report*.

Sobolev, A.V., Hofmann, A.W., Kuzmin, D.V., Yaxley, G.M., Arndt, N.T., Chung, S.-L., Danyushevsky, L.V., Elliott, T.*, et al.* 2007. The amount of recycled crust in sources of mantle-derived melts. *Science*, **316**, 412-417.

Stuckless, J.S. & Ericksen, R.L. 1976. Strontium isotopic geochemistry of the volcanic rocks and associated megacrysts and inclusions from Ross Island and vicinity, Antarctica. *Contributions to Mineralogy and Petrology*, **58**, 111-126, http://doi.org/10.1007/BF00382180.

Stump, E. 1995. *The Ross Orogen of the Transantarctic Mountains*. Cambridge University Press, New York.

Sun, S.S. & Hanson, G.N. 1975. Origin of Ross Island basanitoids and limitations upon the heterogeneity of mantle sources for alkali basalts and nephelinites. *Contributions to Mineralogy and Petrology*, **52**, 77-106, http://doi.org/10.1007/BF00395006.

Takahashi, E. 1986. Origin of basaltic magma-Implications from peridotite melting experiments and an olivine fractionation model. *Bulletin of the Volcanology Society of Japan*, **30**, S17-S40.

Tessensohn, F. & Wörner, G. 1991. The Ross Sea rift system, Antarctica: Structure, evolution, and analogs. *In*: Thompson, M.R.A., Crame, J.A. & Thompson, J.W. (eds) *Geological Evolution of Antarctica*. Cambridge University Press, New York, 273–278.

Thomson, J.A. 1916. *Report on the inclusions of the volcanic rocks of the Ross Archipelago (with Appendix by F. Cohen). Report of the British Antarctic Expedition 1907 - 1909*.

Timm, C., Hoernle, K., Van Den Bogaard, P., Bindeman, I., Weaver, S., 2009. Geochemical Evolution of Intraplate Volcanism at Banks Peninsula, New Zealand: Interaction Between Asthenospheric and Lithospheric Melts. *Journal of Petrology*, **50**, 989-1023.
Tinto, K.J. 2019. Petrogenetic models for the evolution of alkalic magmas in the Erebus volcanic province, Antarctica. *abstract A248 IN: ISAES 2019 : XIII International Symposium on Antarctic Earth Sciences, 22-26 July 2019, Songdo Convensia, Incheon, South Korea*.

Treves, S.B. & Kyle, P.R. 1973. Geology of DVDP 1 and 2, Hut Point Peninsula. Ross Island, Antarctica. *Dry Valley Drilling Project (Northern Illinois University) Bulletin*, **2**, 11-82.

Upton, B.G.J., Downes, H., Kirstein, L.A., Bonadiman, C., Hill, P.G. & Ntaflos, T. 2011. The lithospheric mantle and lower crust–mantle relationships under Scotland: a xenolithic perspective. *Journal of the Geological Society*, **168**, 873-886, http://doi.org/10.1144/0016-76492009-172.

van der Meer, Q.H.A., Waight, T.E., Scott, J.M. & Münker, C. 2017. Variable sources for Cretaceous to recent HIMU and HIMU-like intraplate magmatism in New Zealand. *Earth and Planetary Science Letters*, **469**, 27-41, http://doi.org/https://doi.org/10.1016/j.epsl.2017.03.037.

van der Wal, W., Whitehouse, P.L. & Schrama, E.J.O. 2015. Effect of GIA models with 3D composite mantle viscosity on GRACE mass balance estimates for Antarctica. *Earth and Planetary Science Letters*, **414**, 134-143, http://doi.org/http://dx.doi.org/10.1016/j.epsl.2015.01.001.

Wallace, M.E. & Green, D.H. 1988. An experimental determination of primary carbonatite magma composition. *Nature*, **335**, 343.

Walter, M.J. 2003. 2.08 - Melt Extraction and Compositional Variability in Mantle Lithosphere. *In*: Holland, H.D. & Turekian, K.K. (eds) *Treatise on geochemistry*. Pergamon, Oxford, 363-394.

Warner, R.D. & Wasilewski, P.J. 1995. Magnetic petrology of lower crust and upper mantle xenoliths from McMurdo Sound, Antarctica. *Tectonophysics*, **249**, 69-92, http://doi.org/http://dx.doi.org/10.1016/0040-1951(95)00014-E.

White, W.M. 2010. Oceanic Island Basalts and Mantle Plumes: The Geochemical Perspective. *Annual Review of Earth and Planetary Sciences*, **38**, 133-160, http://doi.org/10.1146/annurev-earth-040809-152450.

Whitehouse, P.L., Bentley, M.J., Milne, G.A., King, M.A. & Thomas, I.D. 2012. A new glacial isostatic adjustment model for Antarctica: calibrated and tested using observations of relative sea-level change and present-day uplift rates. *Geophysical Journal International*, **190**, 1464-1482.

Woodhead, J.D. 1996. Extreme HIMU in an oceanic setting: the geochemistry of Mangaia Island (Polynesia), and temporal evolution of the Cook—Austral hotspot. *Journal of Volcanology and Geothermal Research*, **72**, 1-19, http://doi.org/http://dx.doi.org/10.1016/0377-0273(96)00002-9.

Workman, R.K. & Hart, S.R. 2005. Major and trace element composition of the depleted MORB mantle (DMM). *Earth and Planetary Science Letters*, **231**, 53-72.

Wörner, G., 1999. Lithospheric dynamics and mantle sources of alkaline magmatism of the Cenozoic West Antarctic Rift System. Global and Planetary Change, 23: 61-77.
Wörner, G., Fricke, A., Burke, E., 1993. Fluid inclusion studies on lower crustal gabbroic xenoliths from the Mt. Melbourne Volcanic Field (Antarctica): Evidence for the post-crystallization uplift history during Cenozoic Ross Sea Rifting. European Journal of Mineralogy, 5: 775-785.
Wörner, G. & Zipfel, J. 1996. A mantle P-T path for the Ross Sea Rift margin (Antarctica) derived from Ca-in-olivine zonation patterns in peridotites xenoliths of the Plio-Pleistocene Mt.Melbourne Volcanic Field. *Geol JB*, **B89**, 157-167.

Wright, A.C. 1979a. *McMurdo Volcanics at Foster Crater, Southern Foothills of the Royal Society Range, Central Victoria Land, Antarctica.* New Zealand Geological Survey Internal Report.

Wright, A.C. 1979b. *McMurdo Volcanics northwest of Koettlitz Glacier, Antarctica.* New Zealand Geological Survey. Internal Report.

Wright, A.C. 1979c. *McMurdo Volcanics on Chancellor Ridge, Southern Foothills of the Royal Society Range, Central Victoria Land, Antarctica.* New Zealand Geological Survey. Internal Report.

Wu, B. & Berg, J.H. 1992. Early Paleozoic lamprophyre dikes of southern Victoria Land: geology, petrology and geochemistry. *In*: Yoshida, Y., Kaminuma, K. & Shiraishi, K. (eds) *Recent progress in Antarctic Earth Science. Proceedings of the sixth International Symposium on Antarctic Earth Science*. Terra Scientific Publishing Company Tokyo, 257-264.

Yaxley, G.M., Crawford, A.J. & Green, D.H. 1991. Evidence for carbonatite metasomatism in spinel peridotite xenoliths from western Victoria, Australia. *Earth and Planetary Science Letters*, **107**, 305-317, http://doi.org/http://dx.doi.org/10.1016/0012-821X(91)90078-V.

Bonadiman, C., Nazzareni, S., Coltorti, M., Comodi, P., Giuli, G., Faccini, B., 2014. Crystal chemistry of amphiboles: implications for oxygen fugacity and water activity in lithospheric mantle beneath Victoria Land, Antarctica. Contributions to Mineralogy and Petrology, 167(3): 1-17.

Frost, D.J., McCammon, C.A., 2008. The redox state of the Earth's mantle. Annual Review of Earth and Planetary Sciences, 36: 389-420.

Harte, B., 1977. Rock nomenclature with particular relation to deformation and recrystallization textures in olivine-bearing xenoliths. Journal of Geology, 85: 279-288.

Herzberg, C., 2004. Geodynamic information in peridotite petrology. Journal of Petrology, 45: 2507-2530.

Martin, A.P., Cooper, A.F., Price, R.C., Kyle, P.R., Gamble, J.A., 2021. Erebus Volcanic Province: petrology. In: Smellie, J.L., Panter, K.S., Geyer, A. (Eds.), Volcanism in Antarctica: 200 Million Years of Subduction,Rifting and Continental Break-up. Geological Society, London, Memoirs, pp. M55-2018-80.

Martin, A.P., Price, R.C., Cooper, A.F., McCammon, C.A., 2015. Petrogenesis of the Rifted Southern Victoria Land Lithospheric Mantle, Antarctica, Inferred from Petrography, Geochemistry, Thermobarometry and Oxybarometry of Peridotite and Pyroxenite Xenoliths from the Mount Morning Eruptive Centre. Journal of Petrology, 56: 193-226.

Molzahn, M., Wörner, G., Henjes-Kunst, F., Rocholl, A., 1999. Constraints on the Cretaceous thermal event in the Transantarctic Mountains from alteration processes in Ferrar flood basalts. Global and Planetary Change, 23(1): 45-60.

Pelorosso, B., Bonadiman, C., Coltorti, M., Faccini, B., Melchiorre, M., Ntaflos, T., Gregoire, M., 2016. Pervasive, tholeiitic refertilisation and heterogeneous metasomatism in Northern Victoria Land lithospheric mantle (Antarctica). Lithos, 248: 493-505.

Perinelli, C., Andreozzi, G., Conte, A., Oberti, R., Armienti, P., 2012. Redox state of subcontinental lithospheric mantle and relationships with metasomatism: insights from spinel peridotites from northern Victoria Land (Antarctica). Contributions to Mineralogy and Petrology, 164(6): 1053-1067.

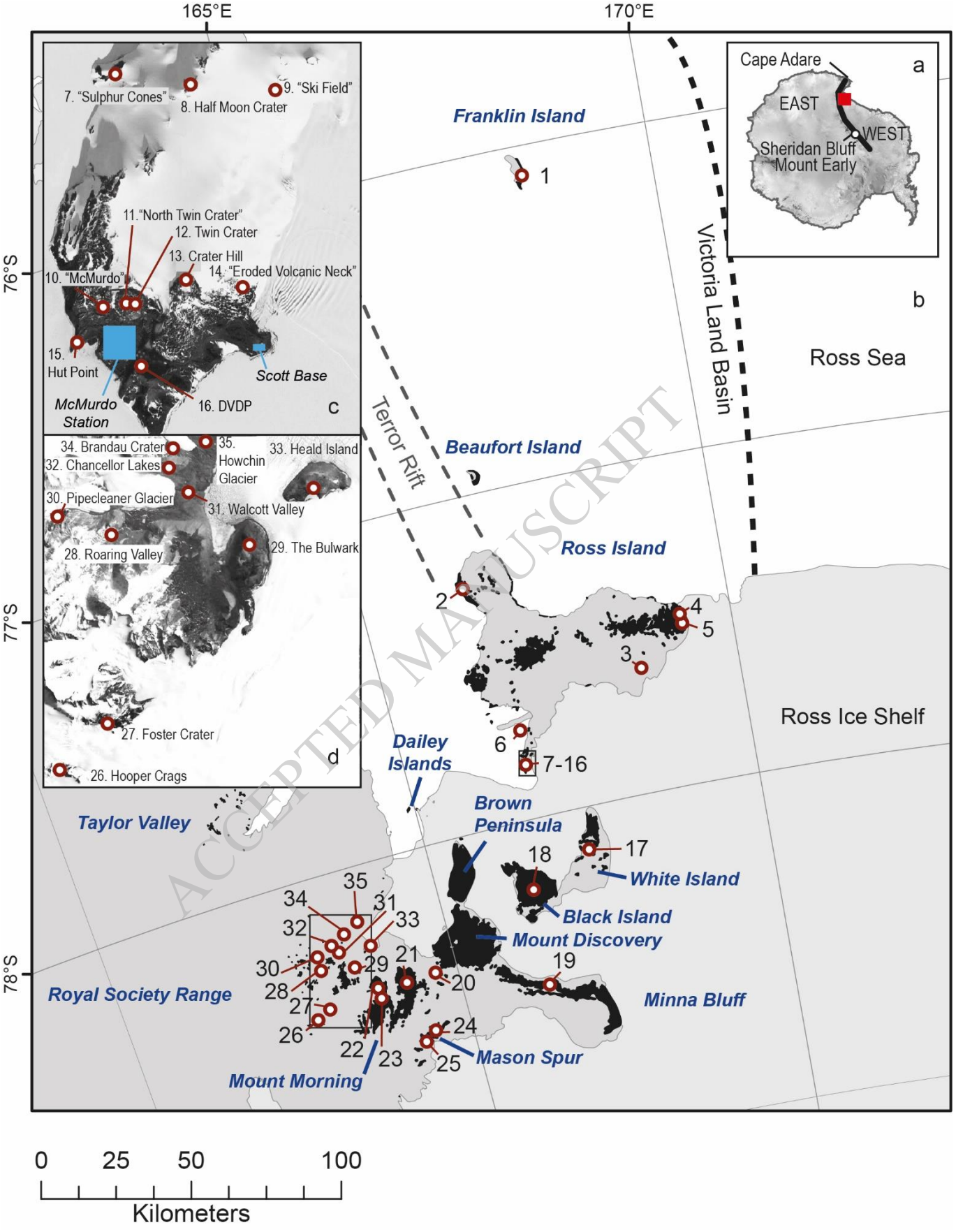

Figure 1 (Intended width 180 mm)

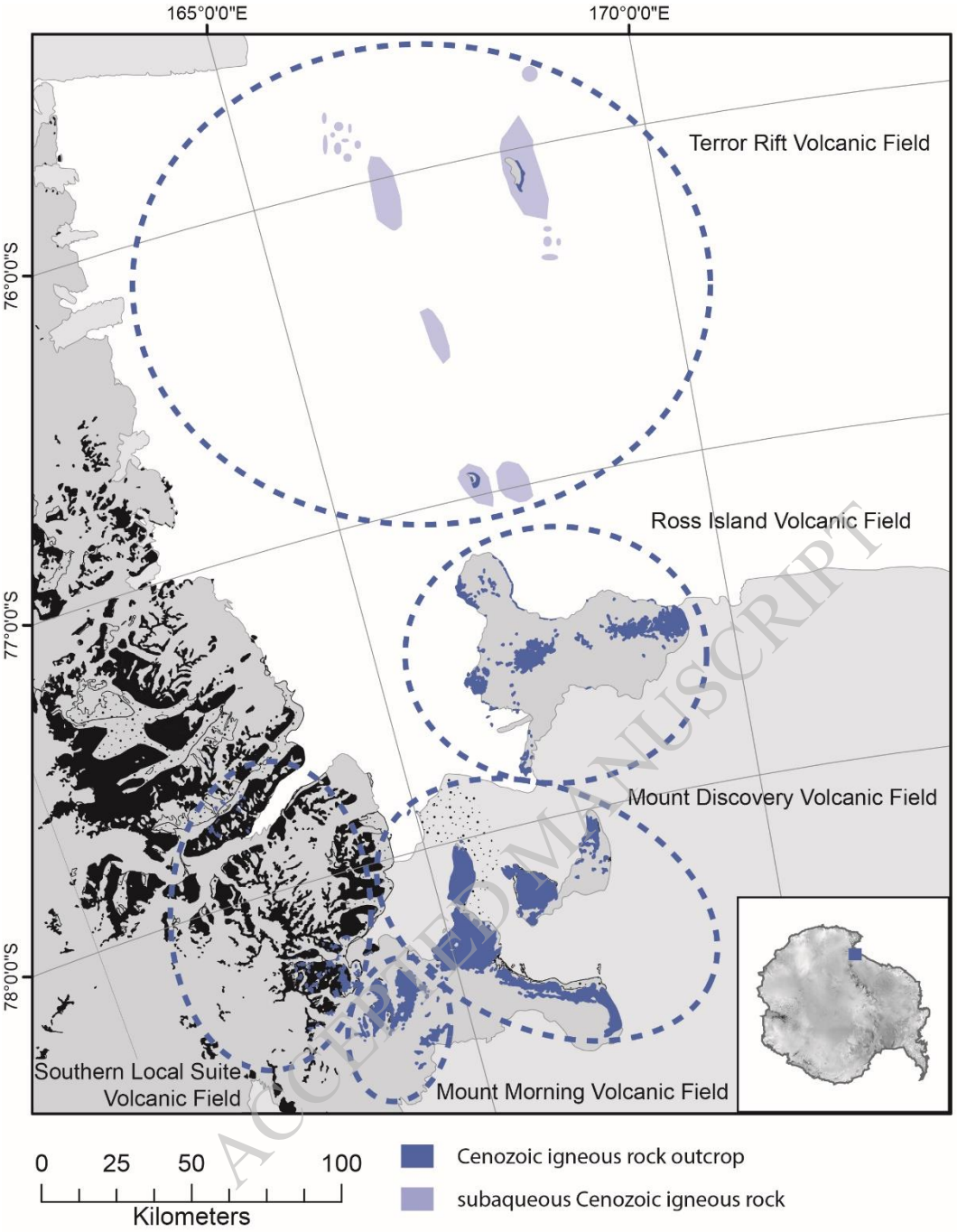

Figure 2 (Intended width 140 mm)

Figure 3 (Intended width 90 mm)

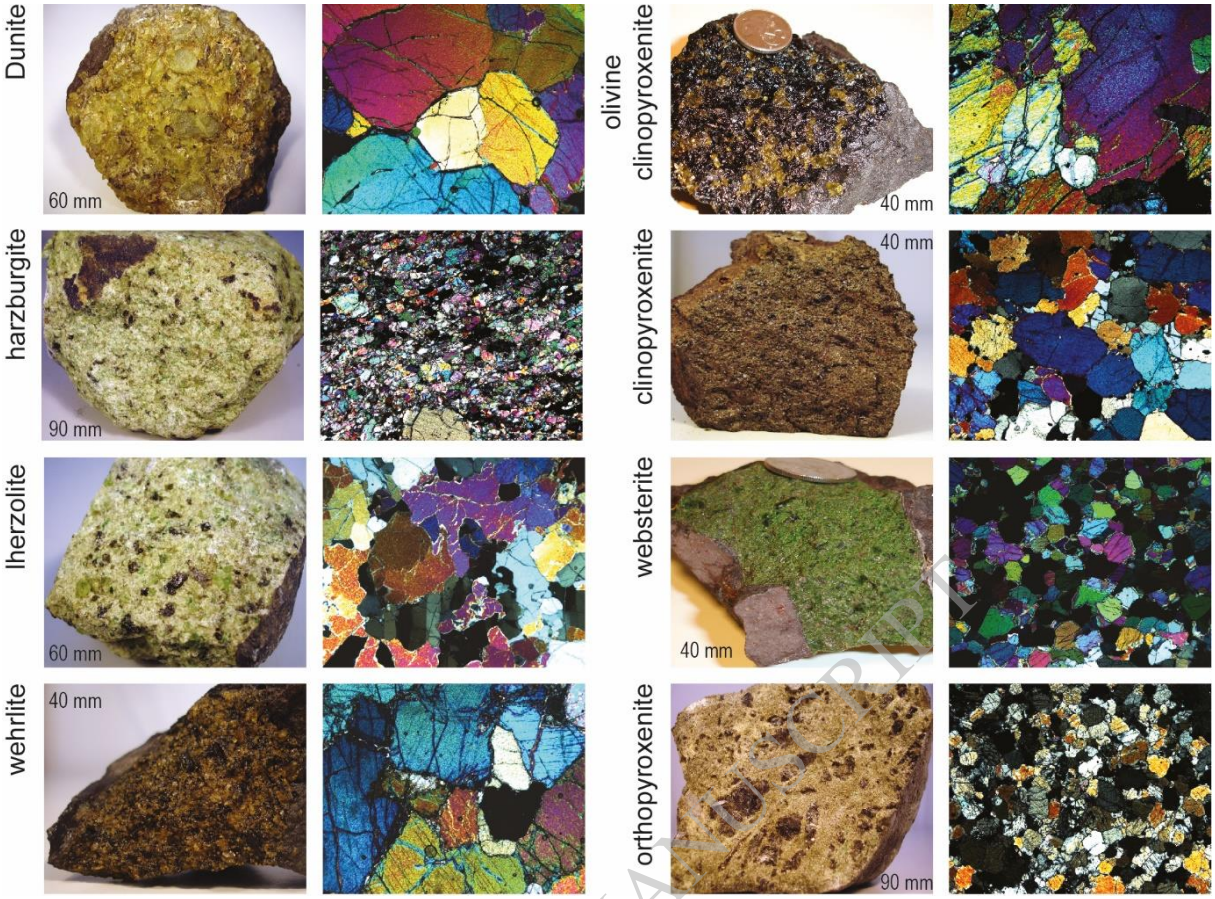

Figure 4 (Intended width 160 mm)

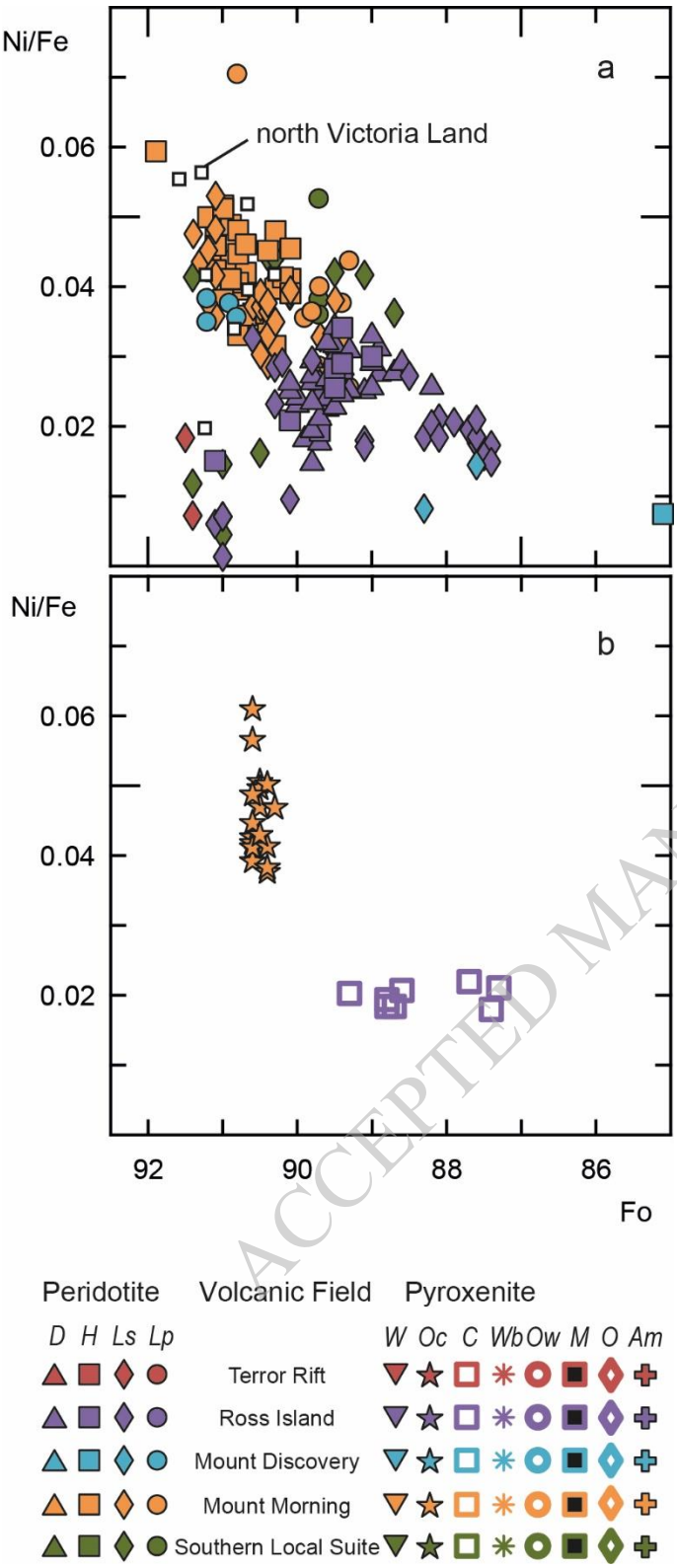

Figure 5 (intended width 90 mm)

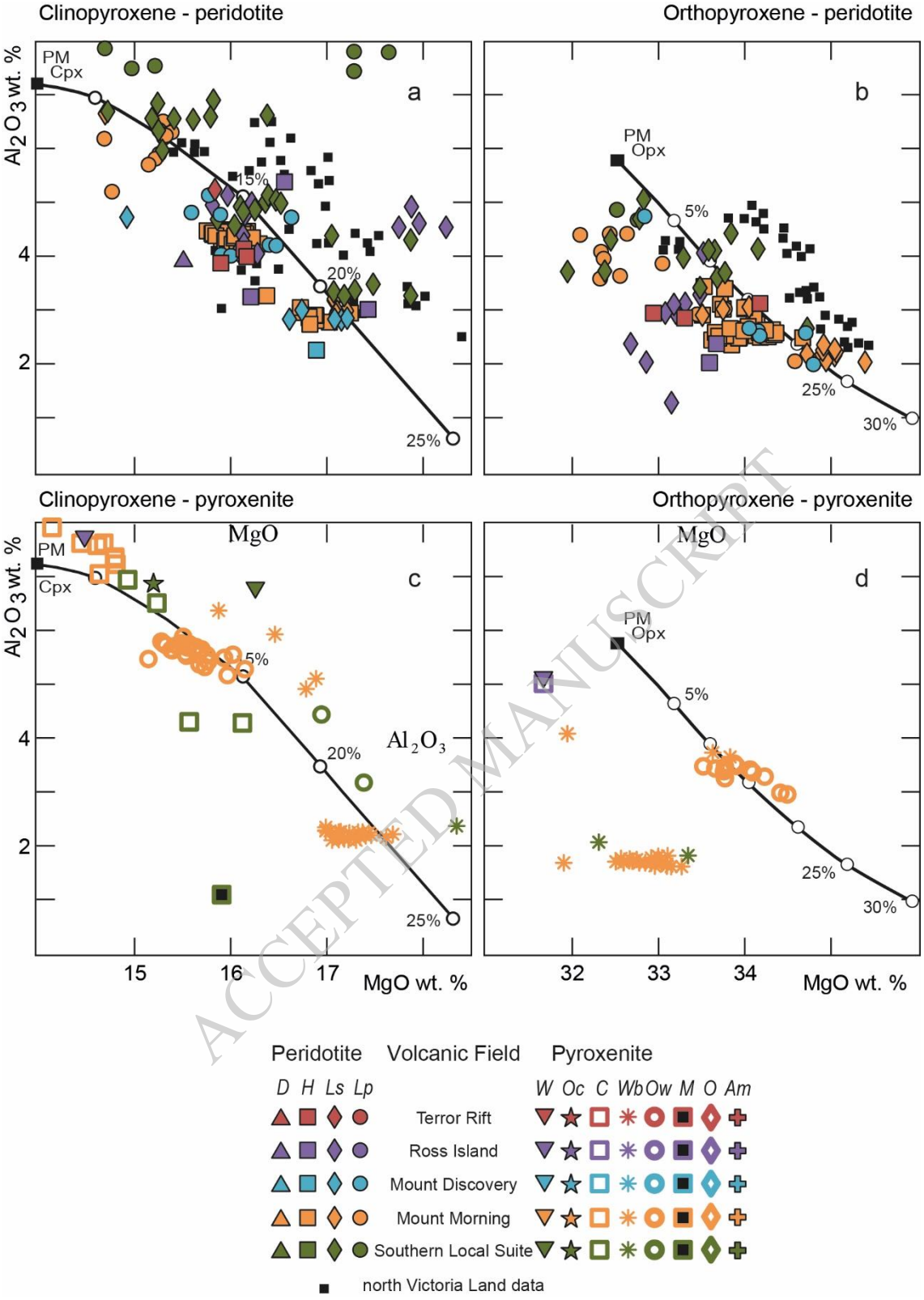

Figure 6 (Intended width 150 mm)

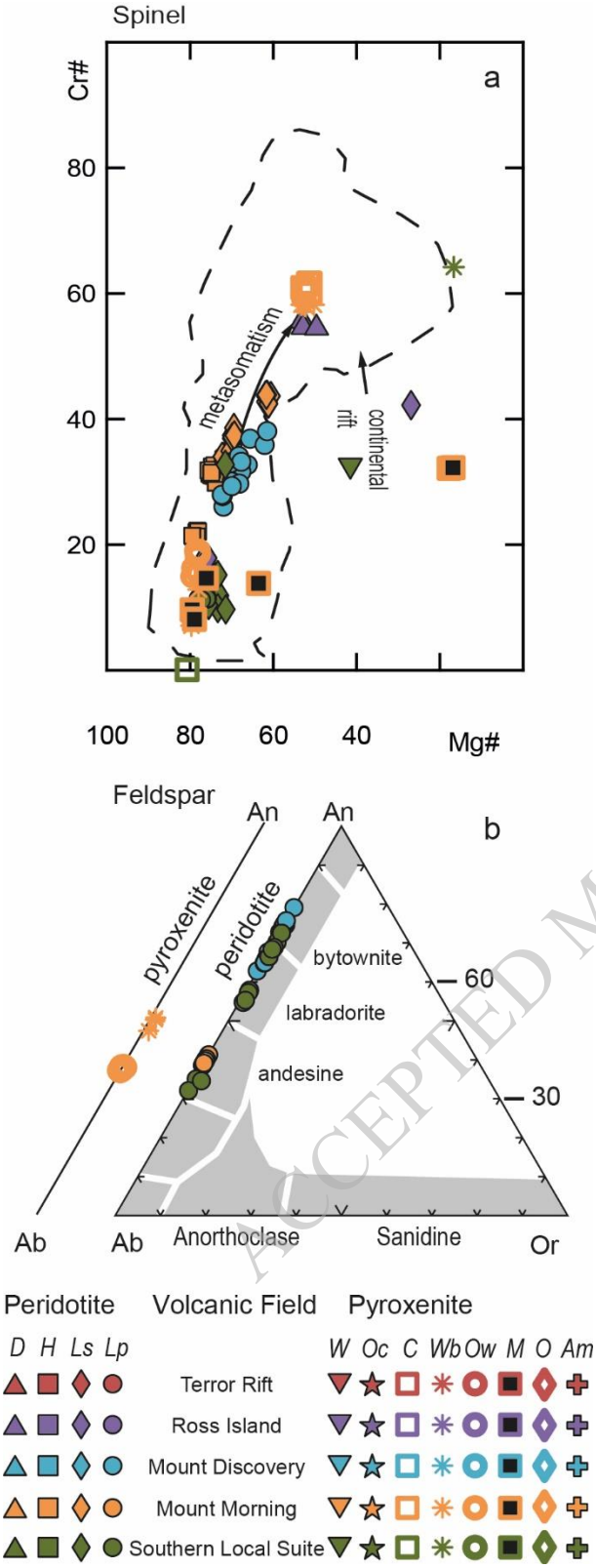

Figure 7 (Intended width 80 mm)

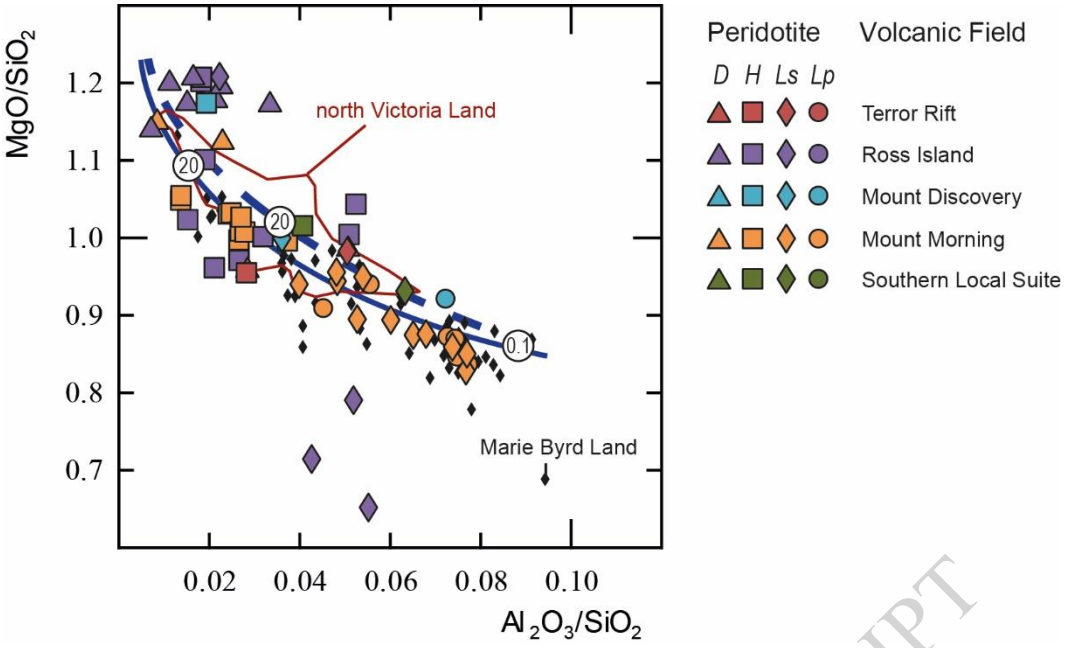

Figure 8 (Intended width 140 mm)

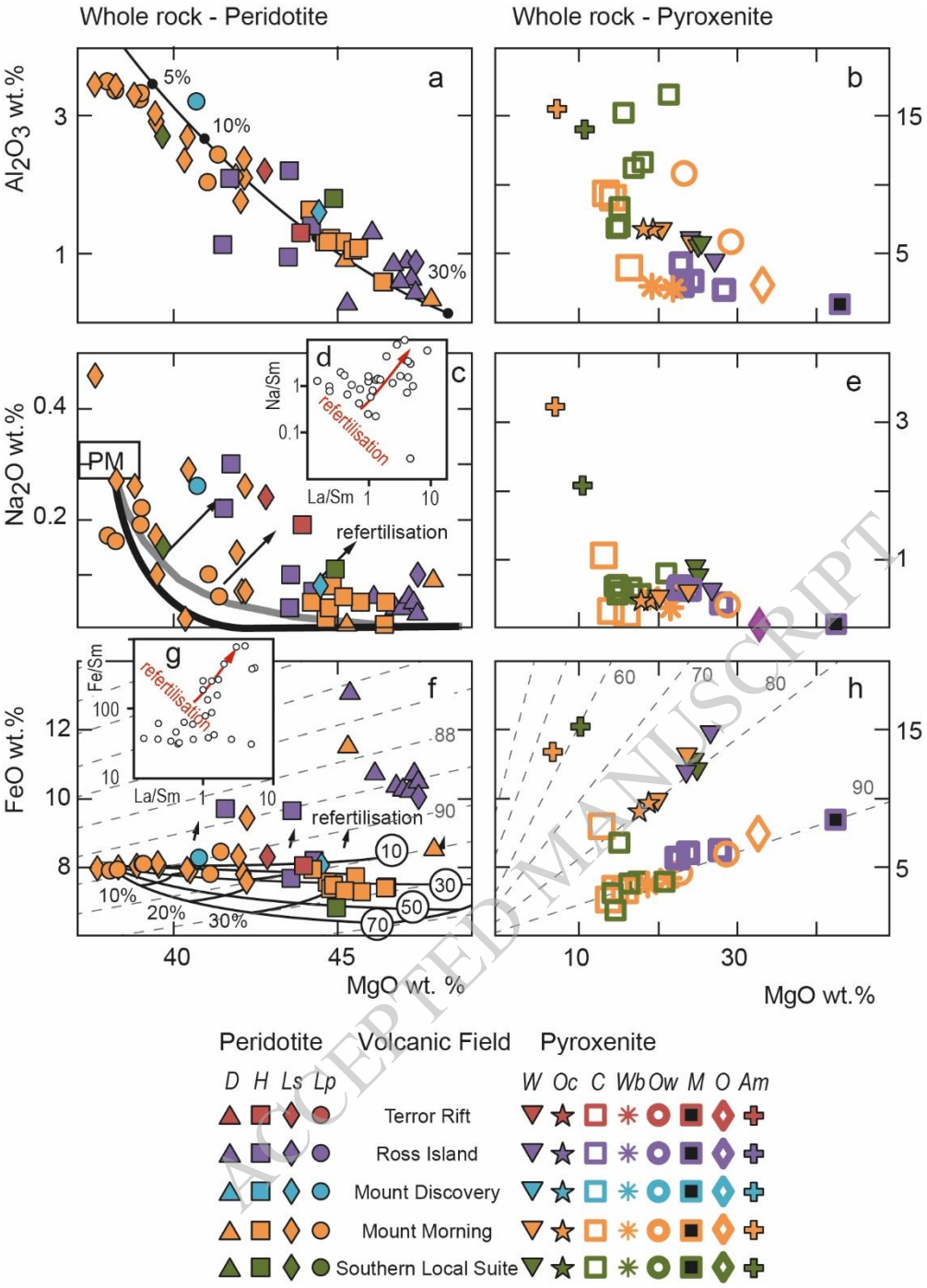

Figure 9 (Intended width 130 mm)

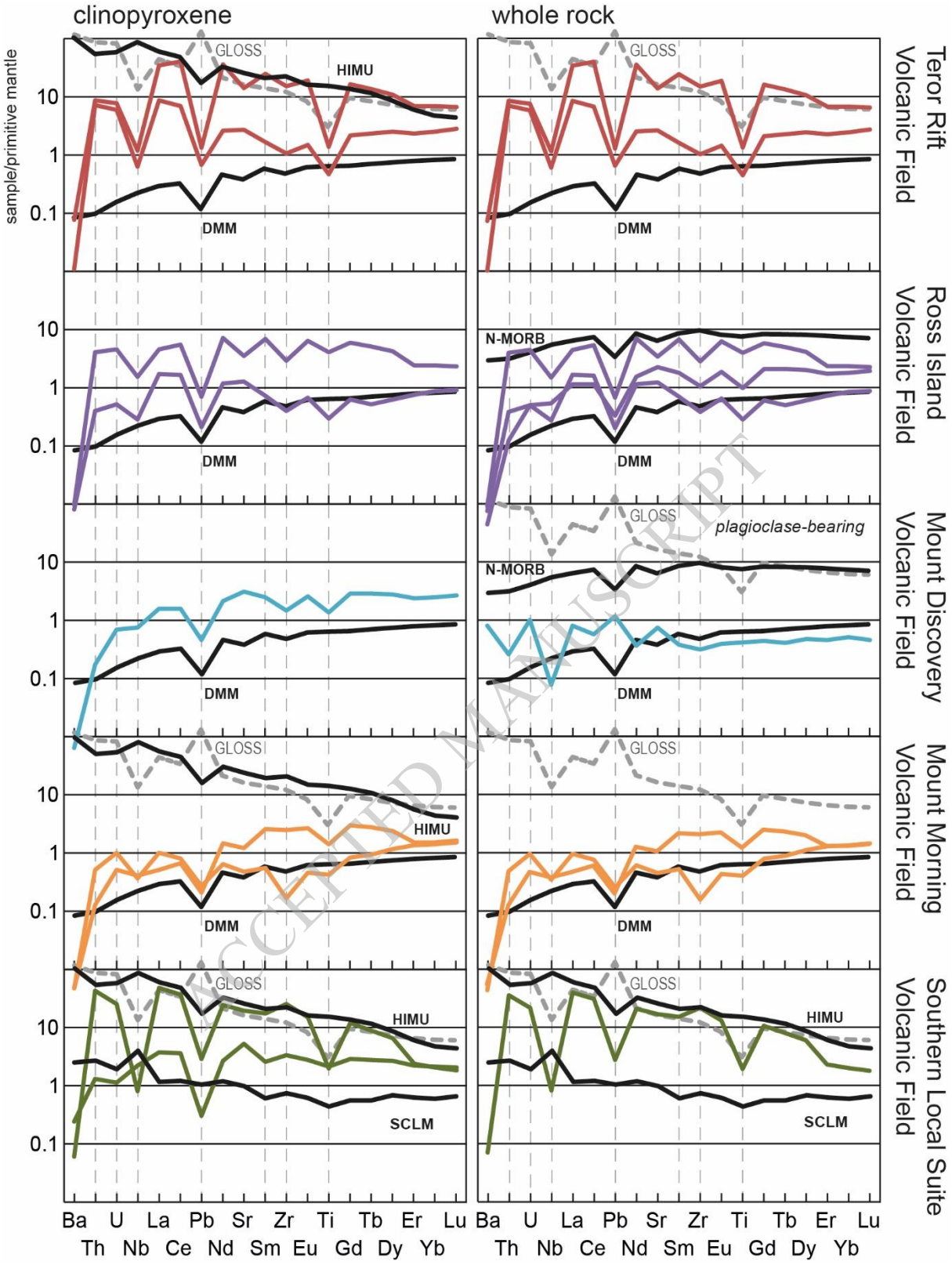

Figure 10 (Intended width 160 mm)

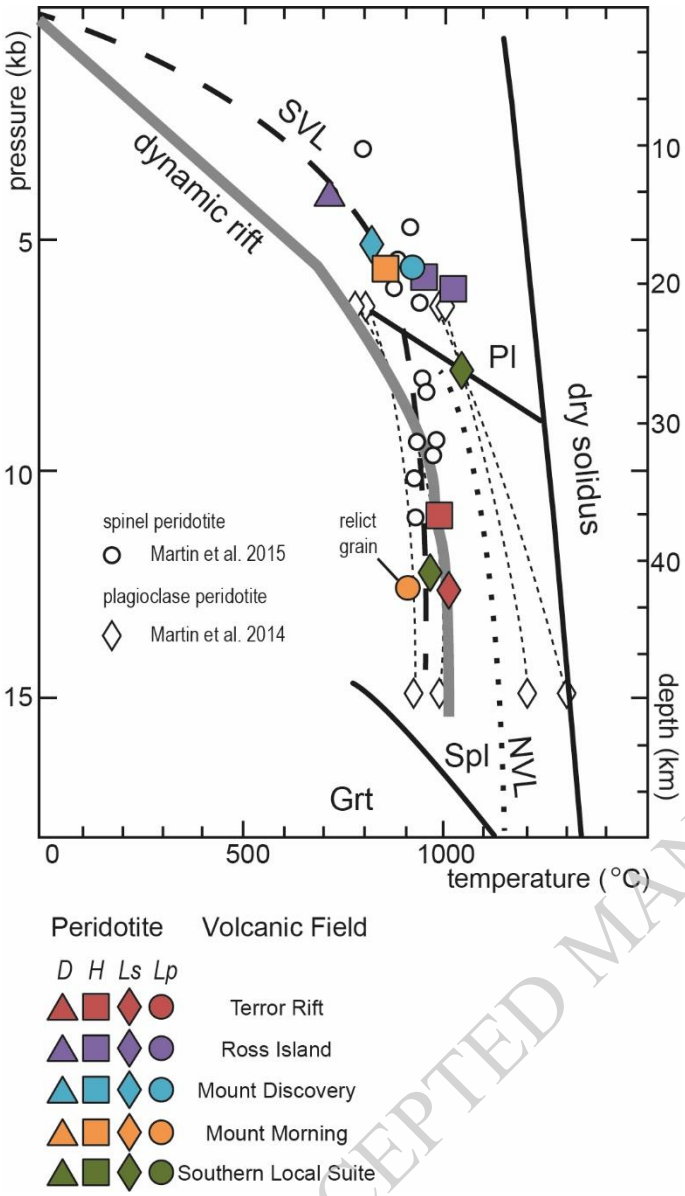

Figure 11 (Intended width 90 mm)

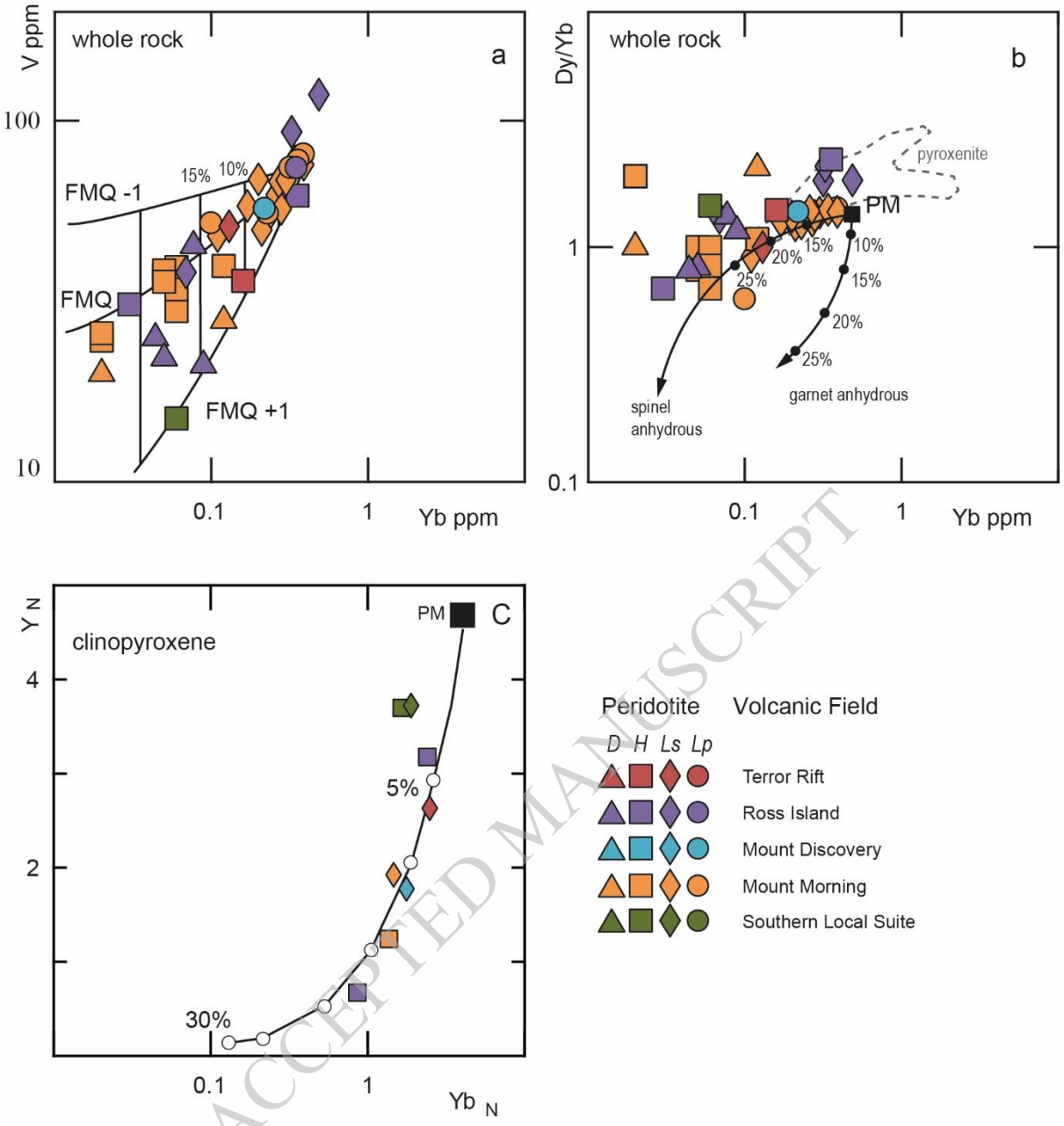

Figure 12 (Intended width 160 mm)

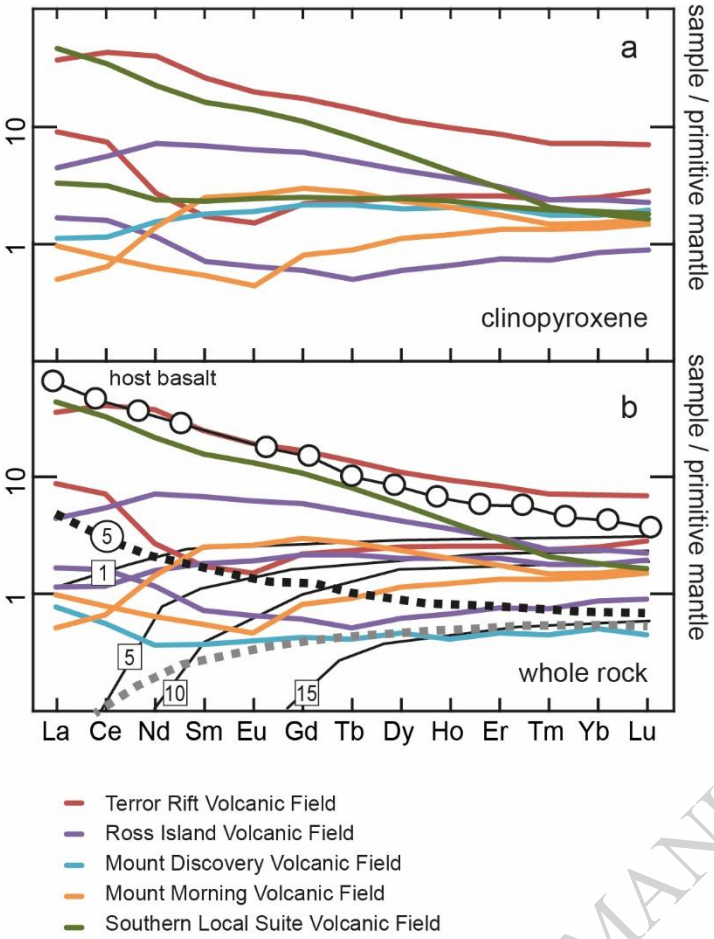

Figure 13 (Intended width 90 mm)

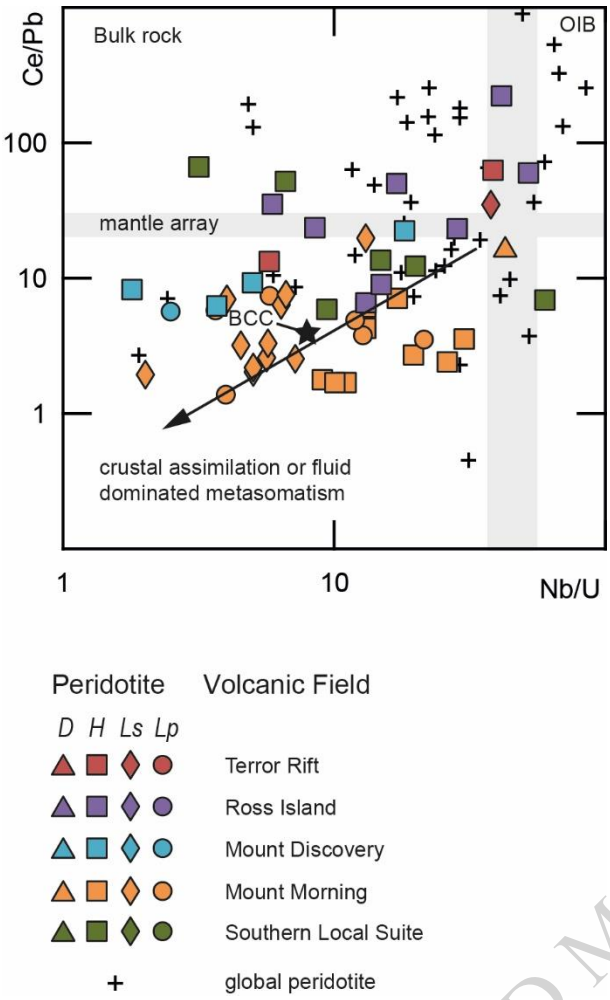

Figure 14 (Intended width 80 mm)

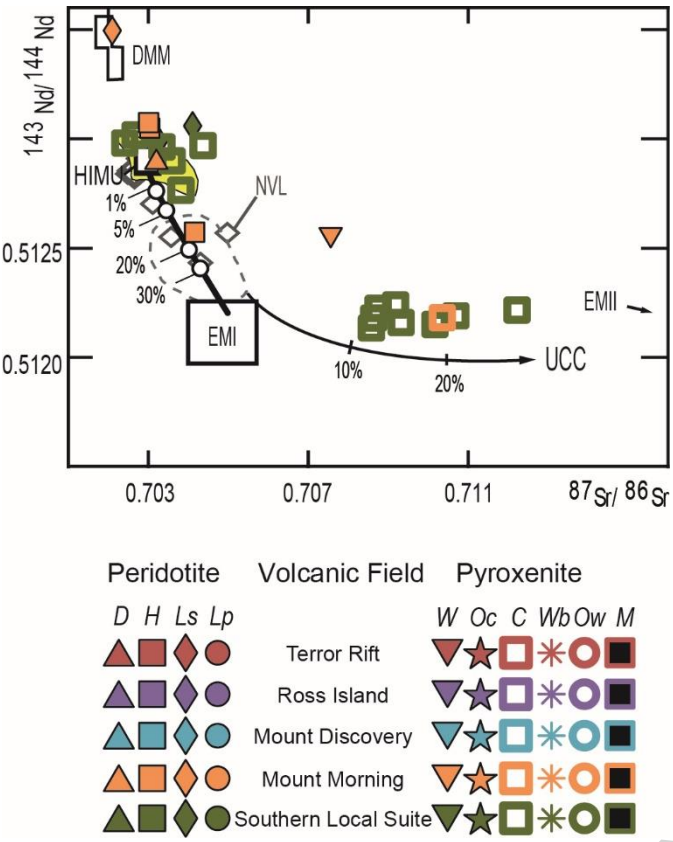

Figure 15 (Intended width 90 mm)

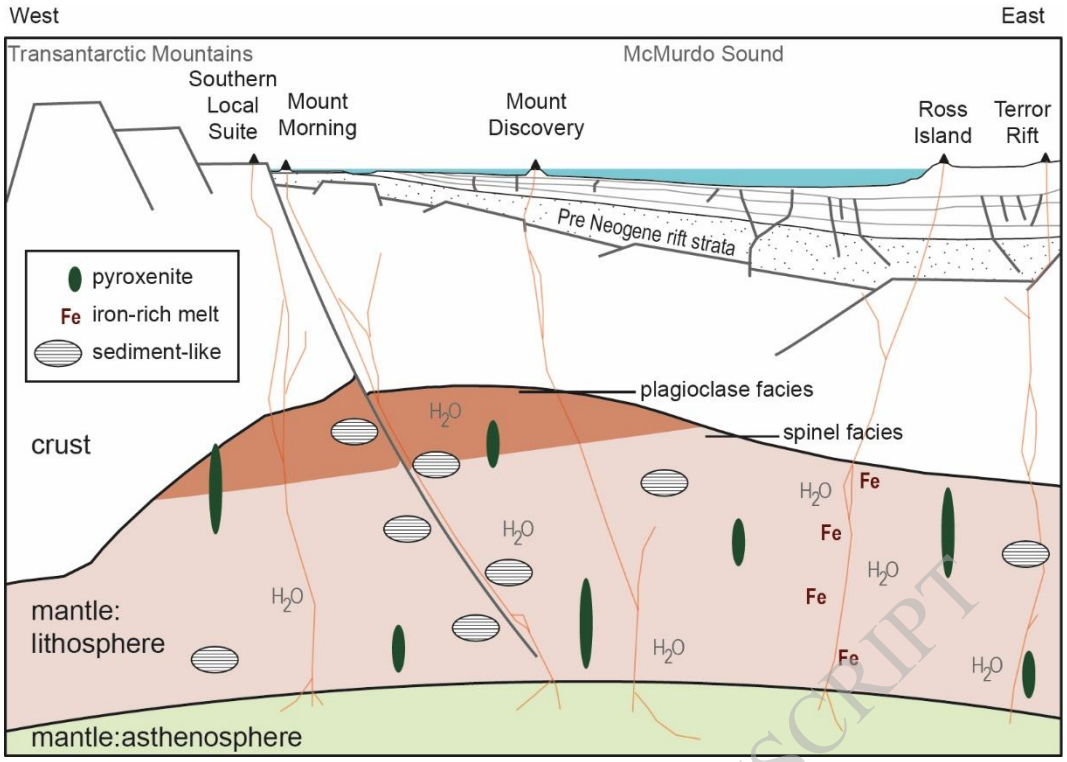

Figure 16 (Intended width 140 mm)